EVALUATING DEFORMABLE IMAGE REGISTRATION FOR CUMULATIVE DOSE ESTIMATION IN GYNECOLOGIC BRACHYTHERAPY

By

Emma Kurth

A THESIS

Presented to the Department of Medical Physics
and the Oregon Health & Science University
School of Medicine
in partial fulfillment of
the requirements for the degree of

Master of Science

June 2025

TABLE OF CONTENTS

Acknowledgements

I would like to express my deepest gratitude to my mentor, Dr. Joe Foy, for his unwavering support, guidance, and encouragement throughout this entire process. His thoughtful feedback, steady mentorship, and genuine investment in my progress made an immeasurable difference in this thesis, and it would not be what it is without him.

I also wish to thank Isaac Bailey and Dr. Byron Wilson for their insightful questions and valuable input, which helped shape and strengthen this project.

To my classmates – thank you for your camaraderie and the many ways we've supported each other. It has made this journey more meaningful.

I am incredibly grateful to my mom for her constant love, support, and encouragement throughout my life and academic path. Thank you for shaping me into the person I am today.

Finally, and most importantly, I want to thank my fiancé, Zach, for being my anchor. Your love, constant reassurance, and endless patience kept me grounded. Your belief in me never wavered, even when my own did, and I am forever grateful for everything you've done to support me – not just during this process, but every step along the way.

List of Abbreviations

Abbreviation	Meaning
AAPM	American Association of Physicists in Medicine
CT	Computed Tomography
CI	Confidence Interval
DIR	Deformable Image Registration
DSC	Dice Similarity Coefficient
DVH	Dose Volume Histogram
EBRT	External Beam Radiation Therapy
EQD_2	Equivalent Dose in 2 Gy fractions
FOV	Field-of-View
HDR	High-Dose-Rate
HR-CTV	High-Risk Clinical-Target-Volume
ICRU	International Commission on Radiation Units and Measurements
HU	Hounsfield Unit
MI	Mutual Information
NCC	Normalized Cross Correlation
OAR	Organ-at-Risk
PDD	Percent-Depth Dose
SSD	Sum of Squared Differences
TG-132	Task Group 132
TRE	Target Registration Error

Abstract

Purpose: Accurate dose accumulation is critically important for precisely evaluating organ-at-risk (OAR) radiation exposure in gynecological brachytherapy. Traditional dose summation methods do not account for spatial variations and may misinterpret cumulative organ doses. Deformable image registration (DIR) provides a unique solution to improve the accuracy of dose mapping. The purpose of this study was to compare the accuracy and clinical impact of DIR-based dose accumulation to simple conventional summation methods for gynecological patients undergoing external beam radiation therapy (EBRT) followed by high-dose-rate (HDR) brachytherapy.

Methods: The retrospective analysis included 10 gynecologic cancer patients treated with EBRT and HDR brachytherapy. Conventionally, cumulative OAR and target doses are estimated by summing dose-volume histogram (DVH) metrics, such as D_{90}, D_{98}, and D_{2cc}, across treatment fractions without accounting for spatial dose variations. This approach assumes a consistent spatial distribution of dose across treatment fractions and ignores anatomical changes that can cause different tissue regions to receive the maximum dose. DIR addresses this limitation by allowing dose to be accumulated spatially. Three DIR algorithms were evaluated: intensity-based, contour-based, and hybrid-based. Accuracy of the registration was quantified with target registration error (TRE) for anatomical landmarks and overlap metrics such as the Dice similarity coefficient (DSC) and Jaccard Index for organ contours. Differences in registration performance were assessed, and dosimetric analyses were statistically compared.

Results: When assessing registration quality, the hybrid-based DIR algorithm had the highest registration accuracy with a mean TRE of 2.71 mm (95% CI: 1.96-3.45 mm), given its use of

intensity- and contour-based information in the DIR-based registration process. The contour-based DIR algorithm had better DSC values, in some cases, when comparing individual structures, but demonstrated poor TRE values, with some as high as 42.5 mm, suggesting that regions without predefined contours were not accurately aligned. The accumulated OAR and regions of interest doses showed that all DIR-based dose summation resulted in lower estimated doses compared to the conservative summation method. Of the structures evaluated, the small bowel and rectum demonstrated a statistically significant difference in dose, with the mean D_{2cc} decreasing by 3.20 Gy (-5.78%) and 2.24 Gy (-3.45%), respectively. The HR-CTV showed a statistically significant D_{90} increase, with a mean of 4.67 Gy (5.49%).

Conclusion: The observed differences may be attributed to high positional and shape variability, suggesting that for highly mobile structures, DIR-based methods may provide a more accurate cumulative dose estimate. Although DIR-based dose accumulation may be more informative when representing cumulative organ doses, its clinical utility is relative to the magnitude of the dose difference. DIR may provide some meaningful benefit for more deformable structures, which may be limited to instances of concern like escalated dose, predisposing gastrointestinal conditions, or greater anatomical variation. Conversely, for more stable structures like the bladder, DIR may not offer an appreciable clinical improvement. Further studies are needed to provide clinical DIR optimization techniques for cases with brachytherapy applicators, as well as to standardize evaluation methods for dose accumulation accuracy.

1. Introduction

Accurate cumulative dose assessment is vital in the practice of radiation therapy, particularly for gynecologic cancer patients receiving a combination of external beam radiation therapy (EBRT) and high-dose-rate (HDR) brachytherapy. These two treatment modalities are delivered over multiple sessions in distinctly different manners with respect to spatial dose distributions: EBRT treats large volumes with uniform doses, while HDR brachytherapy delivers highly localized, high-intensity doses directly near the applicator. Establishing the cumulative dose to both the tumor and surrounding organs-at-risk (OARs) through a multi-modality treatment course requires methods that account for changes in anatomy and differences in the dose delivery across fractions.

Traditionally, cumulative dose assessments use summation of dose-volume histogram (DVH) metrics while relying on the assumption that the spatial locations of the highest dose regions, such as D_{2cc} values for OARs, remain fixed across all treatment fractions. This assumption disregards organ motion and deformation due to tumor volume shrinkage and/or applicator-induced anatomical changes. This could potentially result in inaccurate cumulative dose estimations. This limitation may be amplified in situations involving combined modalities like EBRT and HDR brachytherapy because each treatment modality treats target volumes that vary greatly in size. While the HDR dose hotspots may vary a couple of centimeters, the maximum EBRT dose regions, especially with treatment approaches like nodal boosts or dose painting, can occur in completely different anatomical regions. This suggests that naïve summation of spatially dispersed delivery methods can result in misleading conclusions.

Deformable image registration (DIR) represents one potential solution, allowing for the voxel-wise alignment and registration of images and dose distributions in an anatomically accurate way across treatment fractions. While there are several DIR algorithms available for clinical use including: intensity-based, contour-based, and hybrid-based methods; variability exists in their accuracy and clinical impact. The aim of this study is to evaluate the performance of, and report on different DIR algorithms using MIM Maestro®[1], and to evaluate the influence on the accuracy of dose accumulation associated with gynecologic HDR brachytherapy. By comparing both deformable dose summation and conventional dose summation methods and reporting registration accuracy through overlap-based and landmark-based metrics, key insight was obtained into this determining the feasibility of using DIR and the potential clinical value it provides for cumulative dose evaluation.

1.1. Background

HDR intracavitary brachytherapy is an important part of radiation therapy treatment for gynecological malignancies, particularly cervical and endometrial cancers. HDR brachytherapy typically involves placing a highly radioactive source, such as iridium-192, within or adjacent to the tumor using specialized applicators. HDR brachytherapy provides localized dose distributions with rapid dose fall-off, limiting OAR exposure to the bladder, rectum, sigmoid, and small bowel[2]. The benefit of HDR brachytherapy in terms of local tumor control and overall survival has been well established, and it has become a standard of care as part of EBRT for locally advanced disease[3–5].

In the treatment of many patients with gynecological cancer, the treatment course follows a sequential approach: EBRT is delivered first to target potential microscopic disease within the pelvic and para-aortic lymph nodes, and HDR brachytherapy to deliver a concentrated dose to the primary tumor site[6]. In cases of nodal disease, this is appropriately followed by EBRT boosts to the involved lymph nodes, often delivered as either sequential boosts or as a simultaneous integrated boost[7]. These EBRT boost areas may overlap with the target and nearby OARs such as the small bowel and rectum, contributing to increased cumulative doses in those regions. However, the spatial location of these EBRT hotpots are typically different from those of HDR brachytherapy. As illustrated in Figure 1, EBRT delivers a dose homogeneously over a larger volume while HDR brachytherapy delivers doses locally with significantly larger doses per fractions with steep dose gradients near the source location. With regards to the OARs, these differences have reasonable uncertainty, as does the spatial location of the maximum doses, so dose summation in a direct manner is challenging. Advanced computational dosimetry techniques are therefore essential to analyze cumulative dose distributions.

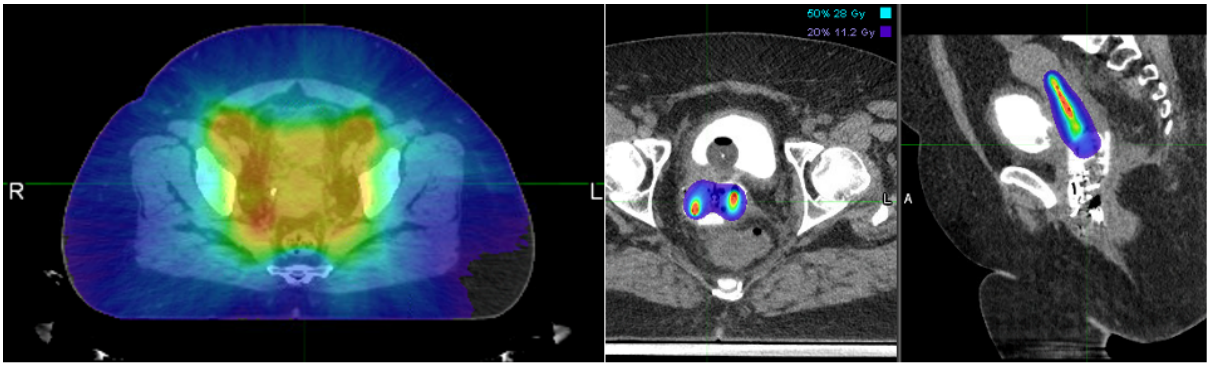

Figure 1 Left: Dose distribution from EBRT; Middle: Axial CT from HDR brachytherapy; Right: Sagittal CT from HDR brachytherapy.

In HDR brachytherapy, the conventional way to assess cumulative dose across fractions is by simply summing dose-volume histogram (DVH) statistics, which provide target metrics, such as D_{90} and D_{98}, and D_{2cc} to organs-at-risk. This approach assumes the spatial stability of maximum dose across fractions, which may not necessarily be aligned with anatomical variation. One method to construct cumulative dose assessment is by using DIR, which allows the mapping of dose distributions on imaging datasets acquired over the entire course of treatment. However, variability may influence DIR accuracy, which is particularly problematic for regions undergoing substantial anatomical changes or near high-dose gradients. This study aims to investigate the validity and effectiveness of DIR-based cumulative dose summation utilizing the MIM Maestro®[1] for HDR brachytherapy in gynecological patients. This method is intended to characterize how robust DIR is for aligning dose distributions spatially, and to expand methods of dose assessment and precision of treatment outcome evaluation.

1.2. Physics of HDR Brachytherapy

As mentioned previously, HDR brachytherapy utilizes a highly radioactive source to deliver precise, high-dose radiation directly to the tumor. The most common radioisotope used in HDR brachytherapy is iridium-192 (Ir-192), with a half-life of 73.8 days, emitting photons with an average energy of approximately 0.38 MeV[8]. HDR brachytherapy photons exhibit a steeper dose gradient with increasing distance from the source, primarily due to the inverse square law, while attenuation in tissue plays a smaller role, and compton interactions dominate at this energy. Although Ir-192 photons undergo some attenuation and scatter in tissue, the steep dose gradient characteristic of HDR brachytherapy is largely a result of geometric factors[9]. This effect is demonstrated in Figure 2, which shows a comparative percent depth dose (PDD) curve of an Ir-

192 source relative to an external 6 MV photon beam. The 6 MV external beam not only deposits dose more uniformly throughout the deeper tissues, but Ir-192 sources have a much steeper dose decline due to its point-source geometry and proximity to the target. This steep dose falloff is advantageous for the sparing of adjacent healthy tissue, but it requires the source to be in a precise location within the applicator in relation to the anatomy to ensure target coverage as expected. While HDR brachytherapy uses radiation sources that are in very close proximity to the patient; therefore, treatment and geometrical dose fall off is much sharper; EBRT treatment uses source locations that are fairly far from the patient in the treatment field, which makes the inverse square effect less significant[10]. Ir-192 is typically encapsulated in a cylindrical container that is about 3.5 mm in length and 0.6 mm in diameter, allowing for accurate positioning in clinical treatment, and for steep dose gradients to effectively confine radiation to the tumor to spare contiguous normal tissues[8,11].

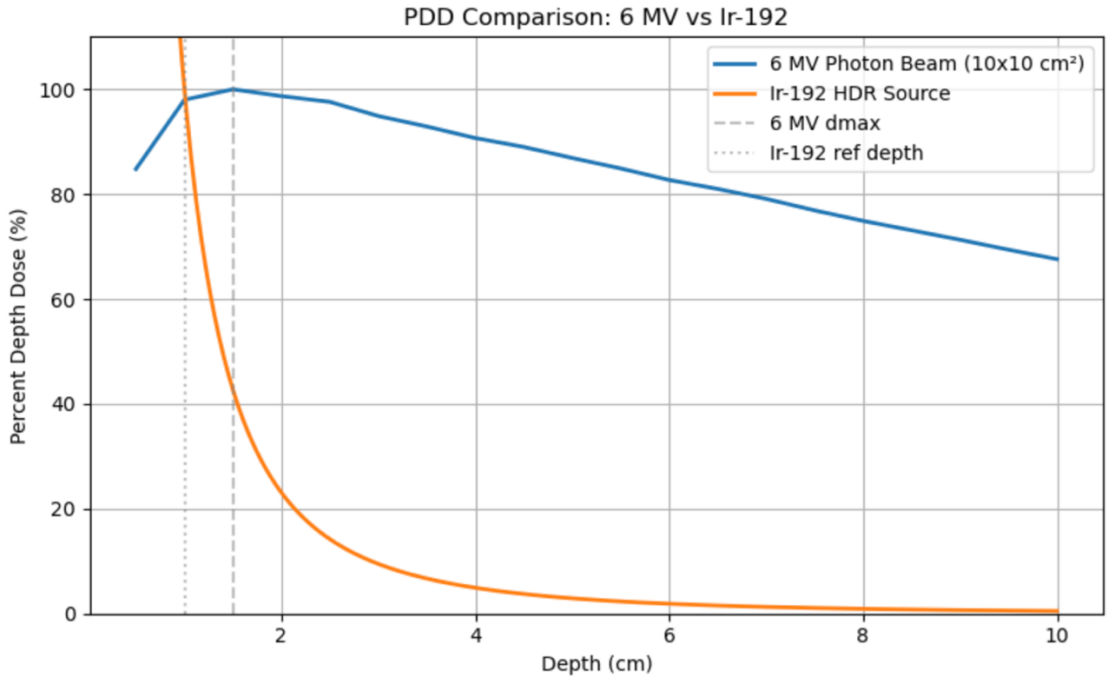

Figure 2 Comparison of percent depth dose (PDD) curves for Ir-192 and a 6MV photon beam (10x10 cm² field size). The Ir-192 PDD is normalized at 1 cm, the reference depth used in HDR brachytherapy, while the 6 MV PDD is normalized at its depth of

maximum dose (d_{max}), 1.5 cm. The rapid dose falloff for Ir-192 highlights the steep dose gradient near the source, in contrast to the more gradual falloff of the 6 MV beam. The 6 MV beam PDD curve was generated using normalized data based on values from: McDermott PN, Orten CG. The Physics & Technology of Radiation Therapy. 2nd ed. Madison, WI: Medical Physics Publishing; 2018.

1.3. HDR Applicators and Treatment Planning

HDR brachytherapy employs a remote afterloading system that advances the radioactive source through a catheter or applicator along a predetermined path. The system allows for dwell positions, which are specific points where the source pauses to deliver radiation, before the source is then moved again. The dwell time at each dwell position is the equivalent of the time the source remains at that position, and it dictates the dose being delivered. The distance between dwell positions, is referred to as the step size and is determined at the time of treatment planning [12,13]. By modifying the parameters of dwell positions and dwell time, treatment planners can create the dose distribution and shape the dose to optimize coverage to the tumor while minimizing toxicity to the OARs. For treatment of gynecological cancers, a few common applicators include intracavitary applicators such as tandem and ovoid (T&O), or tandem and ring (T&R) applicators, both of which are used often for cervical cancer treatments. Hybrid applicators like the Venezia, and Geneva, combine intracavitary components along with optional interstitial needles, which could allow for improved dose conformity in cases with bulky or asymmetric disease[14,15]. When only inserting needles is required and for extensive or parametrial involvement, fully interstitial systems such as the Syed-Neblett template can be used[16]. Treatment planning is typically performed using computed tomography (CT) or magnetic resonance imaging (MRI), which allow for proper placement of the applicator, and delineation of the target and OARs.

1.4. Dose Prescription Guidelines in HDR Brachytherapy

The fractionation and prescribed dose for gynecological malignancies are dependent on both the type of disease and subsequently the applicator used for the treatment of the tumor. For cervical cancer, a typical treatment regimen would include an EBRT course with 1.80 Gy per fraction for 25 fractions (totaling 45 Gy), often followed by 6.00 Gy per fraction for 5 fractions of HDR brachytherapy (30 Gy total)[17]. However, direct dose summation should not be done as there is a gross difference in fraction size and biological effect between EBRT and HDR brachytherapy.

To account for these differences, the Equivalent Dose in 2 Gy fractions (EQD_2) is used. EQD_2 represents the biologically effective dose from different dose fractionation schemes, converted to a common reference of 2 Gy fractions. This allows physicians to assess the cumulative dose to both the tumor and the OARs. EQD_2 is calculated by applying the linear-quadratic model, which describes the biologic effect of radiation by modeling the repair of sublethal DNA damage. The definition of EQD_2 in formula form is seen in Equation 1,

$$EQD_2 = D * \frac{\frac{\alpha}{\beta}+d}{\frac{\alpha}{\beta}+2} \quad (1)$$

where D is the total dose, d is the dose per fraction, and α/β is the tissue-specific radiosensitivity ratio[18].

This adjustment is essential because an individual HDR brachytherapy fraction will have a much greater biological effect than an individual 2 Gy fraction of EBRT. For example, consider 30 Gy delivered in 5 fractions of HDR brachytherapy at 6.00 Gy each. Using the linear-quadratic model with an α/β ratio of 10 (typical for tumor tissues), would correspond to approximately 40

Gy EQD_2. In contrast to the EBRT of 45 Gy delivered in 25 fractions at 1.80 Gy each result in roughly 44 Gy EQD_2. Therefore, although the HDR brachytherapy would have contributed a lower total physical dose, the larger dose per fraction increases its biological effect. The importance of using EQD_2 to properly evaluate and sum the contributions from two separate treatments with these significantly distinct fractionation schemes must be considered, to maintain tumor control and minimize OAR toxicity.

These calculations will use α/β ratios that are selected based on DNA repair mechanisms. Tumors and early-responding tissues typically have higher α/β ratios which indicate less sensitivity toward fraction size; while for late-responding normal tissues, lower values indicate more susceptibility to larger fraction sizes. It is important to note that α/β ratios are not universal. While 10 Gy is often assumed for tumors and 3 Gy is often assumed for late-responding normal tissues like the rectum, bladder, sigmoid, and small bowel, there is variability in these values. Certain tumors, such as prostate cancer, are believed to have α/β ratios much lower and closer to late-responding tissues[19]. Additionally, some normal tissues, such as mucosa or skin, may function more like early-responding tissues where α/β ratios are higher[20]. Therefore, utilizing the appropriate α/β ratio is essential for accurate EQD_2 estimates and proper treatment planning.

To minimize the risk of toxicity to surrounding organs, dose constraints are applied to small high-dose regions, typically quantified as the maximum dose delivered to 2 cm^3 of an organ, termed D_{2cc}. This metric closely reflects the near-maximum dose and has been shown to correlate with late toxicity in brachytherapy. As EQD_2 can meaningfully depict doses of various fractionation schemes on a biologically effective scale, D_{2cc} constraints are expressed in EQD_2 as

well. By converting all delivered doses to EQD_2 using appropriate α/β ratios, physicians can assess what the cumulative dose to each OAR is and whether it is within safe limits. Below in Table 1, are typical EQD_2-based constraints used in gynecological HDR brachytherapy[21,22]:

Table 1 EQD_2-based dose constraints for common organs at risk (OARs) and high-risk clinical target volume (HR-CTV) parameters in gynecological HDR brachytherapy as outlined in the EMBRACE II Study protocol. Constraints are calculated using α/β ratio of 3 Gy for OARs, reflecting their late-responding tissue characteristics, and 10 Gy for target volumes.

Structure	Parameter	Dose Constraint	Typical α/β Ratio (Gy)
OARs			
Bladder	D2cc	< 80 Gy	3
Rectum	D2cc	< 65 Gy	3
Sigmoid Colon	D2cc	< 70 Gy	3
Small Bowel	D2cc	< 70 Gy	3
Target			
HR-CTV	D90	> 90 Gy and < 95 Gy	10
HR-CTV	D98	> 75 Gy	10

These constraints are important in reducing the risk of late radiation toxicity, such as rectal bleeding, fistula formation, bowel obstruction, or bladder dysfunction, significantly impacting a patient's quality of life[23]. Considering tissues in EQD_2 with an α/β ratio of 3 Gy indicates the late-responding nature of normal tissues which may be sensitive to larger doses per fraction like those absorbed in HDR brachytherapy. For tumor tissues, an α/β ratio of 10 Gy can be assumed; representing the early-responding characteristics and indicating that the tissues are relatively insensitive to fraction size. With these values, EQD_2 can account for biological response differences between OARs and tumors in EBRT and HDR brachytherapy combinations.

1.5. Deformable Image Registration for Dose Accumulation

The conventional approach of dose summation between EBRT and HDR brachytherapy is to perform an EQD_2-based summation. However, these summations implicitly assume that the highest dose regions, such as the D_{2cc} volumes for OARs, are delivered to the same anatomical location across all treatment fractions; therefore, they ignore the spatial aspect of the treatment that may be seen in dose distributions between and within modalities. Cumulative dose estimates, particularly in high-dose regions, may especially be inaccurate and do not consider motion by surrounding organs due to applicator placement, or anatomical changes between fractions. Figure 3 illustrates the bladder's maximum dose movement between two treatment fractions. Even when targeting the same anatomical region, changes in organ motion and modified anatomy can yield considerable variations of the spatial location of high-dose regions and highlight the disadvantages in conventional dose summation methods.

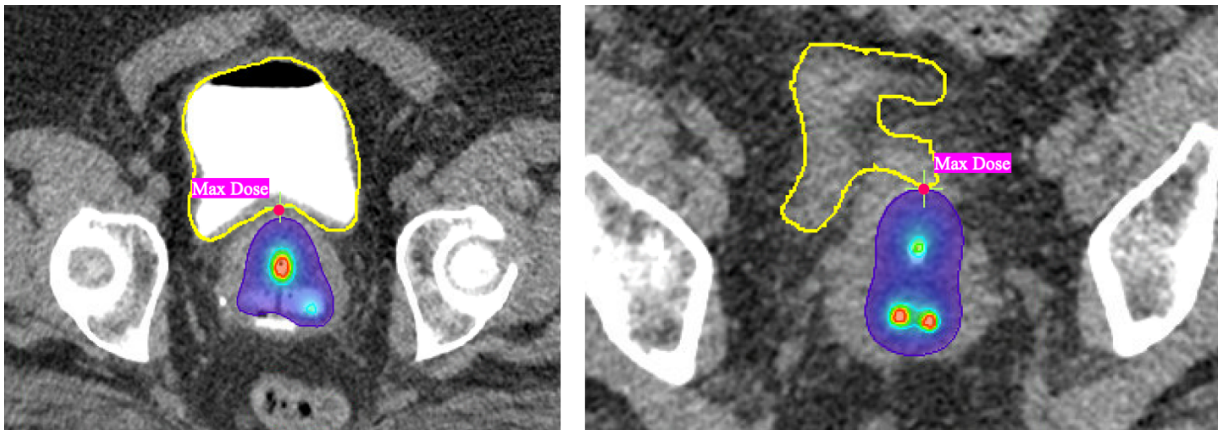

Figure 3 Dose distribution (color wash) within the Geneva applicator from a Fraction 2 CT (left) and a Fraction 4 CT (right). The bladder is contoured, with the maximum dose location indicated in each fraction, demonstrating changes in spatial dose location over treatment fractions.

Using DIR to accumulate dose distributions provides a more accurate representation of the delivered dose by accounting for anatomical changes over time and would eliminate the error associated with considering relying on a single treatment snapshot. DIR allows dose distributions from different imaging datasets to be mapped onto a common anatomical reference frame, which enables voxel-by-voxel dose accumulation. DIR is the process of using mathematical transformations to align images taken at different time points or with different imaging modalities[24]. In the instance of HDR brachytherapy, where imaging and treatment are performed with both EBRT and HDR brachytherapy, DIR can merge these image sets their corresponding dose distributions, ultimately giving a more accurate and precise cumulative dose estimate. DIR approaches can be classified into intensity-based and contour-based methods, and hybrid-based approaches that utilize both options to attain accuracy in dose estimates. Figure 4 shows how DIR maps the rectum contour from the HDR fraction 2 CT onto the HDR fraction 4 CT anatomy, illustrating how DIR accounts for anatomical deformation between fractions. Although DIR has demonstrated promise for cumulative dose estimation, accuracy remains a challenge, particularly in regions with considerable amount of deformation, such as surrounding OARs in the pelvis.

1.6. Deformable Image Registration Algorithms

1.6.1. Image-Based DIR

Image-based DIR is a voxel intensity-driven registration method that aligns images by minimizing differences in grayscale intensity values between corresponding voxels. During the registration process, the algorithm optimizes transformations based on voxel similarity metrics assuming that corresponding anatomical structures maintain correlated intensity values across

different image sets[25]. Common similarity measures used in image-based DIR include mutual information (MI), sum of squared differences (SSD), and normalized cross-correlation (NCC) that guide the algorithm to achieve spatial alignment of the images based on image content rather than features defined by the user[26].

In MIM, image-based DIR is implemented using a free-form deformation model guided by voxel intensity information. This technique performs best when the images are from the same modality (e.g., CT to CT) and acquired under similar imaging conditions[27,28].

There are several limitations to this method, particularly in cases of significant anatomical deformations, organ filling variations, or changes in patient positioning[27,29]. Since image-based DIR relies only on voxel intensity information without incorporating anatomical structure guidance, it may struggle to maintain structural integrity when aligning highly deformable regions, such as the bladder, rectum, or small bowel[30,31]. Because these organs may experience significant volumetric and shape changes between fractions of HDR brachytherapy, intensity-only registration would likely be prone to inaccuracies without additional anatomical guidance.

1.6.2. Contour-Based DIR

Contour-based DIR relies on user-defined anatomical structures (contours) to guide deformation, aligning corresponding structures across datasets by minimizing surface discrepancies. Contour-based DIR does not rely on voxel intensities; instead, it seeks a spatial alignment between structures, deforming the image to match in shape and location to contours from a reference dataset[26].

In MIM, the contour-based DIR algorithm deforms the displacement vector field so that contour surfaces align while interpolating the transformation across adjacent image regions. This method is especially beneficial in cases of inconsistent image quality or mismatched modalities where intensity values may not reliably indicate structure boundaries[28].

Contour-based DIR does have limitations, particularly with poor initial contour agreement, missing structures, or inconsistencies in mutual segmentations[30]. If the contours are inaccurate or incomplete and do not include the anatomical features of interest, registration error will likely arise. Furthermore, since contour-based DIR does not consider or use voxel intensity information, it may struggle in areas where intensity-based DIR could otherwise enhance registration accuracy[29,30].

1.6.3. Hybrid-Based DIR

Hybrid-based DIR integrates both voxel intensity information and anatomical contour information to provide a more balanced and anatomically accurate registration, particularly in cases where significant deformation is present[26]. Hybrid-based DIR combines the benefits that intensity-based DIR offers, and the contour information established from manually segmented structures.

Hybrid-based DIR proceeds as follows in MIM, where DIR uses a cost function, comprising of two components: a similarity term ($C_{similarity}$) and a smoothness term (C_{smooth}). These two are weighted through a weighting factor (λ), which defaults to 0.5 [27]:

$$Cost = C_{similarity} + \lambda C_{smooth} \quad (2)$$

The similarity term ($C_{similarity}$) minimizes differences between the primary and secondary images based on voxel intensity values, using sum of squared differences, and incorporates differences between the signed distance functions of user-defined contours. The regularization term (C_{smooth}) promotes smoothness in the deformation field, avoiding unrealistic transformations[28].

Hybrid-based DIR allows for the combination of intensity-based information and contour-based constraints into the optimization process, which provides a more anatomically accurate registration, particularly useful in pelvic radiotherapy where organs like the bladder, rectum, and small bowel undergo large, complex deformation processes.

To better illustrate the impact of DIR, a visual example of DIR applied to the rectum across brachytherapy fractions is shown in Figure 4. The original rectal contour from the HDR Fraction 2 CT is compared with the native contour on the HDR Fraction 4 CT, and the deformed HDR Fraction 2 rectum is shown overlaid on the HDR Fraction 4 CT. This demonstrates how MIM's hybrid-based DIR algorithm adapts anatomical structures to account for inter-fractional motion and deformation, particularly in proximity to the applicator.

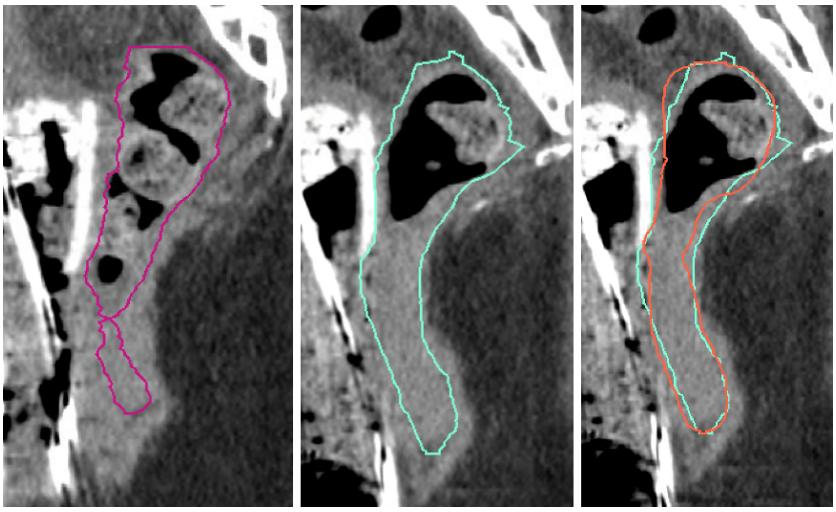

Figure 4 Illustration of deformable image registration (DIR) applied to rectal anatomy between HDR brachytherapy fractions. (Left) HDR Fraction 2 CT with original rectum contour (magenta). (Middle) HDR Fraction 4 CT with original rectum contour (cyan). (Right) HDR Fraction 4 CT with overlaid HDR Fraction 2 CT rectum after DIR (orange) and HDR Fraction 4 CT rectum (cyan). The overlay demonstrates how DIR modifies structure shape and location to account for anatomical deformation between treatment fractions.

1.7. Prior Work in DIR-Based Dose Accumulation

Prior studies have assessed DIR in gynecological brachytherapy, indicating both limitations and benefits relative to cumulative dose estimation. One study by Mohammadi et al[27]. evaluated a hybrid-based DIR algorithm for cumulative dose to the bladder and rectum for cervical cancer patients receiving HDR brachytherapy, in comparison to the simple summation approach suggested by The Groupe Européen de Curiethérapie (GEC) and the European Society for Radiotherapy & Oncology (ESTRO)[32]. The study found DIR produced lower accumulated dose estimates compared to simple summation; however, the study recognizes the limitations, including in regions with steep dose gradients and the underlying assumption that the entire planned EBRT dose was uniformly received by the OARs as prescribed.

In a separate comparative study, Zhao et al.[33] investigated the feasibility of DIR to characterize the cumulative dose distributions to organs at risk in patients treated with combined EBRT and HDR brachytherapy for cervical carcinoma. They did not find a statistically significant difference between the cumulative doses calculated using DIR and the direct addition method; they do report that direct addition dose at times overestimated DVH metric parameters. They studied the contribution of DIR in estimating dose accounting for anatomical change and enhancing accuracy of a cumulative dose. The authors do acknowledge that image registration uncertainties during DIR may cause cumulative dose estimates to be inaccurate.

Millar et al.[34] provided further evidence of this by using deformable registration to evaluate the accuracy of International Commission on Radiation Units and Measurements (ICRU) point doses, which are standard dose reporting points defined by the ICRU, and volumetric doses to the bladder and rectum in cervical cancer patients receiving EBRT with multiple fractions of HDR brachytherapy. The findings indicated that cumulative dose estimates to OARs summed based on rigid registration or no registration exhibited substantial variability from deformable summation methods. In most instances, summing physical doses without accounting for anatomical variation led to overestimation of cumulative dose, therefore it was evident that deformable techniques are more accurate methods for dose accumulation. That said, the authors relied on the first HDR brachytherapy CT as the reference image for deformable registration, so their ability to account for anatomical changes between fractions was likely limited over the various fractions of treatment.

Building on this work, the goal of this study is to further evaluate the use and effectiveness of DIR-based cumulative dose summation using MIM and more specifically, the validity and accuracy of the technique in gynecological HDR brachytherapy. Although direct dose summation and rigid registration remain important, many studies have demonstrated the practical advantages of DIR in clinical settings. This study compares multiple DIR methods, such as image-based, contour-based, and hybrid-based approaches, within the same clinical software environment. The important aspects of this work include using the DIR process to map EBRT dose distributions to a single reference HDR brachytherapy image to add patient-specific consideration to the accumulation of dose; and to assess the spatial accuracy of the deformation, this study includes the use of landmark-based evaluations using anatomical landmarks of the patient and features of the applicator.

By refining DIR techniques and validating the accuracy in relation to the high-dose volumes of gynecological cancer treatment, this study aims to enhance the clinical utility of DIR-based cumulative dose assessments. Overall, the objective is to improve current methods of dose accumulation to allow for better assessment of OAR exposure, which leads to safer, more individualized treatment planning.

2. Methods

2.1. Patient Data

This study utilized 10 anonymized CT datasets from patients diagnosed with gynecological cancer for whom EBRT was delivered followed by HDR brachytherapy. Patients were treated using a Geneva applicator, as depicted in Figure 5, with varying numbers of interstitial needles. The number of interstitial needles used varied both across patients, as well as within a patient across treatment fractions.

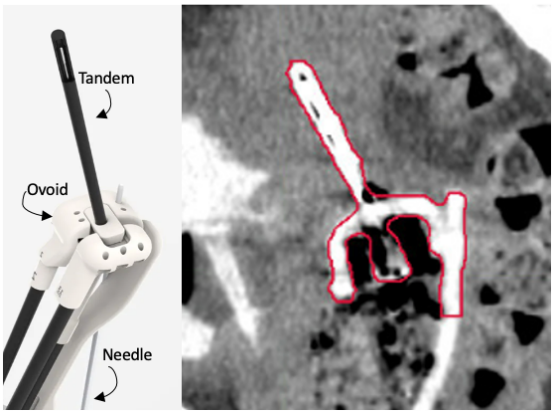

Figure 5 Annotated depiction of a Geneva Applicator. (Left) Diagram showing labeled components of the applicator: tandem, ovoids, and interstitial needles. (Right) Corresponding CT slice with applicator visible and contoured (red)[35].

Each patient completed five CT scans: the first scan necessary for EBRT treatment planning and the last four CT scans corresponded to the individual HDR brachytherapy fractions. EBRT planning is typically performed on a single scan due to it being resource intensive, the low doses delivered per fraction, and the larger treatment volumes which allow for the assumption of limited anatomical variability during the course of treatment. In contrast, for HDR brachytherapy with the Geneva applicator, a new plan is created for each fraction due to the high dose per fraction, steep

dose gradients, and relative proximity of highly radiosensitive and anatomically variable OARs, which all rely on precise, fraction specific imaging. For DIR comparisons, the CT from the fourth brachytherapy fraction (denoted CT_HDRFx4_n) was selected as the primary reference dataset, as it provides the most recent anatomical state before the images are aligned and their dose distributions are combined using DIR-based accumulation. All CT scans were obtained using a standardized imaging protocol, when possible, to ensure consistency across imaging sessions. While the four brachytherapy scans were all acquired with similar imaging protocols, EBRT planning scans were often obtained at external institutions, introducing variability in imaging technology, acquisition parameters, and patient positioning. This variability, combined with anatomical differences introduced by the absence of a brachytherapy applicator, could contribute to greater uncertainty in DIR and cumulative dose estimates, particularly when EBRT doses are ultimately mapped onto brachytherapy imaging. The four HDR brachytherapy CT scans were obtained at a tube voltage of 120 kVp and slice thickness of 1 mm; to provide high spatial resolution for precise dose mapping. The field of view (FOV) was individually adjusted for each patient to produce the clearest images possible while accommodating the entire target volume and surrounding OARs. Typically, the FOV extended laterally to the iliac crest, with the superior boundary positioned approximately 5 to 10 cm above the tip of the applicator, as the inferior boundary extended to the labial level. Imaging was performed with the applicator in place for each HDR brachytherapy fraction to accurately capture potential source positions relative to patient anatomy.

2.2. Treatment Prescription

All patients received an EBRT dose of 45 Gy delivered in 25 fractions, with a fractional dose of 1.80 Gy per fraction. Following EBRT, an HDR brachytherapy boost was administered, delivering a total dose of 28 Gy in four fractions, with each fraction contributing 7.00 Gy. The cumulative dose assessments account for the total dose delivered to the high-risk clinical target volume (HR-CTV) and all OARs contributions from EBRT and HDR brachytherapy. The HR-CTV represents the gross tumor volume and all regions with suspected microscopic disease, including the entire cervix, residual tumors and involved parametrial tissues, as defined at the time of HDR brachytherapy[36].

In accordance to the EMBRACE II Protocol[22] planning aims, D_{2cc} dose constraints were set at 80 Gy EQD_2 for the bladder, 65 Gy EQD_2 for the rectum, and 70 Gy EQD_2 for both the sigmoid colon and small bowel, with higher limits permissible in specific clinical context. Given there are no guarantees that the maximum dose to the OARs will remain in the same location across fractions, DIR is necessary to accurately map dose distributions and evaluate cumulative exposure to both tumor and normal tissues.

2.3. Contouring

The contours were vital to this study in a few ways: for measuring deformable image registration accuracy through overlap-based metrics, and to support dose accumulation analysis with dose-volume histogram metrics (DVH). The DVH metrics were based on predetermined dose

constraints and allowed for a standardized assessment of cumulative dose from both the EBRT and HDR brachytherapy fractions.

Accurate contouring is essential for DIR and dose accumulation because it defines the parts of the anatomy used for registration evaluation and radiation treatment planning. On every CT scan, the OAR contours, namely the bladder, rectum, sigmoid, small bowel, and HR-CTV, were contours that a radiation oncologist approved prior to treatment. These physician-approved contours remained unchanged throughout the registration process to ensure consistency in evaluation. All contouring followed the EMBRACE II protocol, which outlines detailed recommendations for target and OAR delineation in cervical cancer patients. Essentially, the following is true in defining the outer contour of each organ: the bladder includes the entire organ and bladder neck; the rectum is contoured from the ano-rectal sphincter to the recto-sigmoid junction; the sigmoid from the recto-sigmoid junction to the left iliac fossa; and the small bowel encompasses the outer contour of all small bowel loops, including mesentery. There are some structures such as the femoral heads, kidneys, spinal cord, duodenum, and ovaries that may be contoured if needed per EMBRACE II protocol guidelines, especially in cases involving para-aortic irradiation or ovarian transposition[22].

For the EBRT scans, which came from separate referring institutions, contour availability and naming conventions varied. While many structures were available, only those overlapping the HDR brachytherapy defined HR-CTV were used to perform dose accumulation analyses. In particular, the focus was on the portion of the EBRT planning target volume (PTV) that corresponded to the 45 Gy prescription and spatially intersected the HR-CTV from the HDR

brachytherapy plans. This process allowed for a consistent evaluation of cumulative doses across both modalities despite contouring variability between treatment phases.

The primary contouring task done for this study was contouring the brachytherapy applicator for each HDR brachytherapy fraction CT scan. The applicator was contoured using MIM's thresholding tool, which segments structures based on Hounsfield unit (HU) values. A spherical region of interest was placed over the applicator tip, and the HU value ranges were manually adjusted until the high-density applicator material was fully highlighted. This was repeated in several regions along the applicator to ensure full coverage, as minor HU variations between slices sometimes required localized adjustments. With the semi-automated thresholding process, applicator contours could be completed consistently and reproducibly between the HDR fractions. After thresholding was applied, the smoothing tool was chosen to refine the contour and remove any irregularities caused by noise or segmentation artifacts. To maintain clinical relevance, the applicator contour was delineated to approximately 1 cm below the ovoids, as seen in Figure 6, focusing on the region most relevant for dose calculations and registration accuracy assessments.

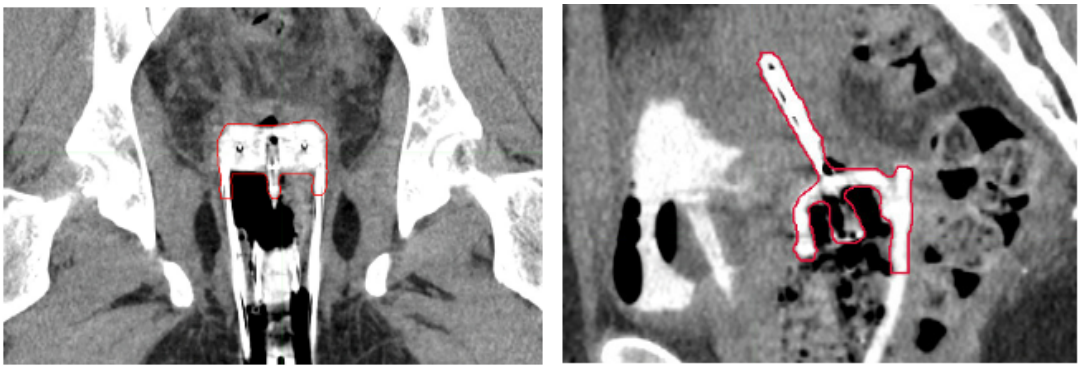

Figure 6 Coronal CT image (left), Sagittal CT image (right) showing the contoured Geneva applicator (red) extending approximately 1 cm below the ovoids.

2.4. Registration Accuracy

Before dose accumulation can take place, it is essential to first evaluate the accuracy of the deformable image registration, as any inaccuracies in the deformation can lead to incorrect spatial mapping of dose. To ensure the reliability of the accumulated dose distributions, DIR accuracy in MIM was assessed using anatomical landmarks representative of the pelvic region, following the recommendations outlined in the American Association of Physicists in Medicine (AAPM) Task Group Report 132 (TG-132)[37]. The anatomical landmarks consisted of bony structures such as the femoral heads, iliac crests, and sacroiliac joints, as well as treatment-specific points, including the bladder catheter entrance and components of the Geneva applicator. The identified landmarks were chosen for their consistent visibility across CT images and relevance in assessing spatial alignment within the pelvic anatomy, particularly in the context of cumulative dose evaluation.

2.4.1. Target Registration Error

Target registration error (TRE) is an extensively recognized metric of accuracy when assessing the performance of deformable image registration algorithms. It reflects the error between corresponding landmarks or anatomical structures across registered images. The calculation involves determining where specific points, such as anatomical landmarks, are located in both the reference and deformed images, measuring the Euclidean distance between their mapped locations. A smaller TRE indicates a higher degree of alignment, reflecting that the registration algorithm has successfully transformed one image to align with the other[38,39]. The formula for TRE can be expressed as:

$$TRE = \sqrt{(x_r - x_m)^2 + (y_r - y_m)^2 + (z_r - z_m)^2} \quad (3)$$

where (x_r, y_r, z_r) represent the coordinates of the reference landmark on the reference image, and (x_m, y_m, z_m) denote the coordinates of the corresponding landmark in a CT image from another treatment fraction after DIR. In summary, a smaller value of TRE indicates better alignment[39]. However, TRE is limited, since it only measures registration accuracy at discrete, user-defined landmarks. These landmarks are typically selected in anatomy with clear anatomical visibility, which may not reflect the registration accuracy in areas with less distinct or more complex anatomy[39]. Despite these limitations, TRE remains a valuable and simple metric for understanding the overall alignment quality on deformable image registrations.

In this study, TRE was used to evaluate the DIR accuracy at anatomical landmarks on stable bony structures and the bladder catheter entrance. The first and second brachytherapy fraction CTs were selected for comparison to evaluate DIR accuracy in a controlled and consistent manner to minimize variability that could arise from cumulative anatomical changes over the course of treatment. Identifying two temporally adjacent HDR brachytherapy fractions, allowed for assessment of the algorithm's performance in a scenario with relatively minor inter-fraction changes, providing a baseline understanding of DIR behavior under favorable conditions. While DIR accuracy may vary with greater anatomical changes, such as those seen when registering EBRT to HDR images, this initial analysis focuses on a more homogeneous case to isolate algorithm performance before exploring more complex scenarios.

By analyzing these values, the effectiveness of different DIR approaches in aligning key anatomical structures was assessed, providing insight into the precision of cumulative dose summation in gynecological HDR brachytherapy.

2.4.2. Dice Similarity Coefficient and Jaccard Index

The Dice Similarity Coefficient and Jaccard Index are metrics that evaluate the overall overlap between segmented structures in two images, providing information about spatial agreement after deformable registration. Both indices assign a numerical value to describe the degree of overlap between two sets, often computed by evaluating regions of interest in the reference image against the registered images. The DSC index is computed by taking twice the area of the overlap between two structures and dividing it by the total area of both structures. The equation for DSC is:

$$DSC = \frac{2|A \cap B|}{|A| + |B|} \quad (4)$$

where A and B represent the sets of voxels of the reference and registered structures, and $|A \cap B|$ is the number of voxels in the intersection of the two sets[40,41]. Equation 4 yields a value between 0 indicting that the structures do not overlap at all, while a DSC of 1 suggests perfect overlap.

The Jaccard index is similar to the DSC, but the index evaluates overlap for the union of the two structures:

$$Jaccard\ Index = \frac{|A \cap B|}{|A \cup B|} \quad (5)$$

where $|A \cup B|$ is the area of the union of the two sets. The DSC index tends to be more sensitive to smaller structures, while the Jaccard index may evaluate overlap more conservatively. For visual reference, Figure 7 illustrates graphically how the DSC is calculated, including a comparison to the Jaccard Index.

Though useful, these metrics have limitations. They primarily assess structural alignment but do not provide any information about local deformations or voxel-wise accuracy, meaning that even a high overlap score does not necessarily equate to correct anatomical correspondence at a smaller scale. Additionally, these metrics do not provide an evaluation for registration accuracy beyond the contoured structures, and their reliability can be affected by variability or inconsistencies in contouring techniques[40,41].

The DSC and Jaccard Index were calculated to evaluate the alignment of key anatomical structures including the bladder, rectum, sigmoid, small bowel, HR-CTV, and applicator (when present), by comparing the reference image (CT_HDRFx4_n) to the CT images from HDR fractions 1-3 and the EBRT planning CT. The DSC and Jaccard Index were recorded for each anatomical structure, so their respective values could be compared between timepoints, and the performance of DIR in maintaining anatomical consistency was quantitatively assessed. This analysis plays a critical role in validating the reliability of cumulative dose estimation, which directly depends on the anatomical accuracy of the underlying image registration.

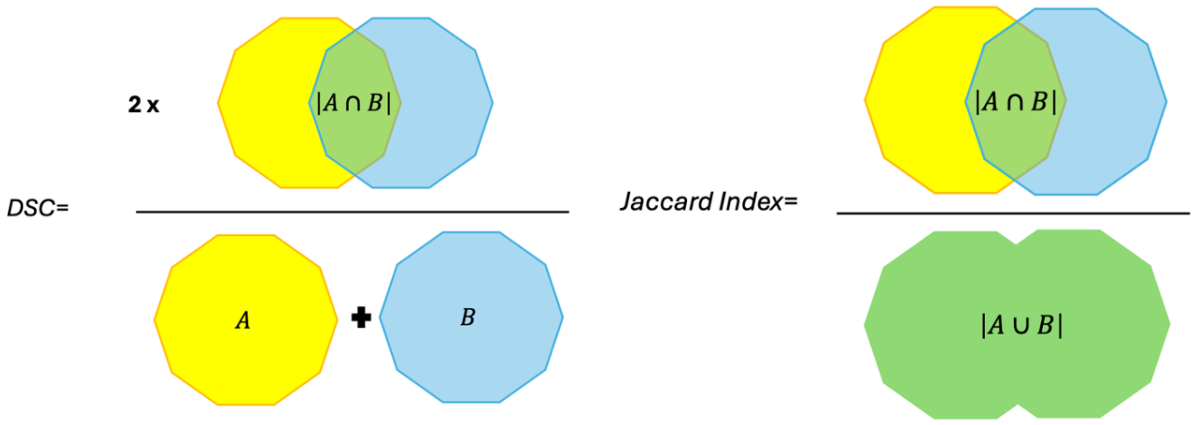

Figure 7 Graphical Illustration of Dice Similarity Coefficient and the Jaccard Index calculation. Adapted from Al Rahamneh et al. (2021).

2.5. Justification for Metric Selection

While TG-132 outlines multiple evaluation metrics, including Jacobian determinant analysis, inverse consistency error, and mean distance to agreement (MDA), this study focused on measures most directly applicable to clinical dose assessment. TRE was selected, as it quantifies spatial alignment using anatomical landmarks, a critical factor when assessing the reliability of dose deformation. DSC and Jaccard Index were additionally used to assess contour overlap due to their established use in radiotherapy and their relative robustness to small contouring variations.

Other metrics were excluded based on practical limitations or limited clinical relevance. The Jacobian determinant and inverse consistency error focus on mathematical properties of the deformation field, which do not indicate dosimetric accuracy[42,43]. MDA was not used due to its heightened sensitivity to contour boundary inconsistencies, which can be pronounced in highly deformable structures[44].

2.6. Deformable Registration Workflow

Deformable image registration was performed to align and analyze cumulative doses across multiple CT datasets. The registration consisted of a defined process workflow (Figure 8) and was initiated by specifying primary and secondary image series. The first level of registration was accomplished using point-based rigid registration, which in this case included a selection of landmarks located within the applicator. Rigid registration uses translations and rotations to bring the landmark points into correspondence without changing the original image geometry. Once this alignment was complete, the second level of registration was to perform deformable registration. The study used three types of DIR algorithms: image-based DIR, contour-based DIR, and hybrid-based DIR. The accuracy achieved by the DIR process was quantified with TRE, DSC and the Jaccard Index to assess anatomical agreement. Following deformation, the images were visually inspected for registration errors and artifacts before proceeding with dose mapping.

The workflow includes optional steps for Reg Refine® and Reg Reveal®. These tools were not systematically applied due to the high variability in their impact on different registrations. Reg Reveal® provides a visualization tool to compare the deformed and original images, helping assess the quality of the registration and identify areas that may require refinement. Reg Refine® allows for localized manual adjustments to the deformation map, enabling correction of specific misalignments without altering the entire registration[30]. To assess whether localized refinements could improve dose accuracy, Reg Refine® was selectively applied to three patients who initially demonstrated an unexpected increase in dose after DIR. All other DIR results and analyses presented in this study were conducted without the use of Reg Refine® or Reg Reveal®, to ensure that the central conclusions reflect the default performance of the DIR algorithms in MIM.

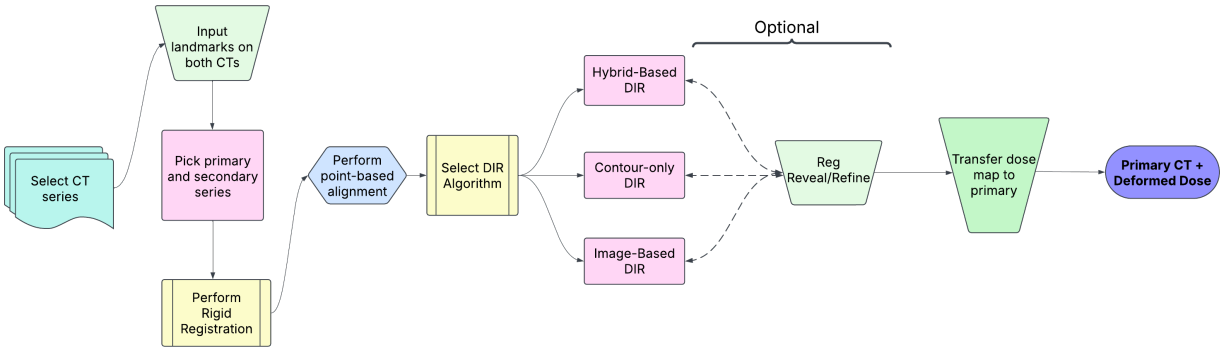

Figure 8 Workflow for the deformable image registration process in MIM, incorporating setting landmarks for alignment and the optional refinement process.

For EBRT-HDR registrations, a primary challenge encountered was the presence of a Geneva applicator in the HDR brachytherapy images, which was absent in the EBRT datasets. TG-132[45] notes that most DIR algorithms assume smoothness in the vector field, therefore when there exists a singularity – such as the introduction of an applicator – registration errors can occur. In planning to address this, anatomically stable landmarks were placed on bony structures visible in both EBRT and HDR scans, including the symphysis pubis, femoral heads, and iliac crest. The landmarks were used both during the DIR process to guide alignment, assess registration accuracy, and for dose deformation, since their anatomical consistency across EBRT and HDR brachytherapy images provided a robust reference while remaining distant from the deformation artifacts near the applicator region.

For HDR-HDR registrations, where all CT datasets contained the applicator, two distinct landmark strategies were employed depending on the purpose. For evaluating registration accuracy and calculating overlap metrics, landmarks were placed on consistent anatomical structures such

as bony anatomy and points away from the applicator, to ensure that evaluations were free from potential biases related to applicator-induced deformation. For dose deformation and summation, landmark placement was moved into the applicator itself. This change allowed the deformation algorithm to prioritize alignment in the high-dose region, which is clinically critical for accurate cumulative dose estimation. Registration errors in these high-dose regions were minimized by anchoring the deformation around the applicator leading to more reliable dose accumulation.

2.7. Spatial Tracking of Maximum Dose Location

To quantify anatomical variability and spatial displacement across fractions, the movement of the maximum dose location for each structure was measured using Euclidean distances. Because coordinate systems between scans weren't inherently aligned, a rigid registration task was first performed between image sets. The EBRT scan was rigidly registered onto HDR Fraction 1 using bony anatomy for alignment, and for HDR fractions, a series of rigid registrations were performed using applicator-based landmarks: HDR fraction 2 to HDR fraction 1, HDR fraction 3 to HDR fraction 2, and HDR fraction 4 to HDR fraction 3. After registration, the maximum dose voxels were manually localized for the bladder, rectum, sigmoid, small bowel, and HR-CTV, and their (x, y, z) coordinates were recorded. Euclidean distances between maximum dose coordinates from one fraction to the next were then calculated to assess the amount of spatial movement. The Euclidean distance formula in 3D space goes as follows:

$$Distance = \sqrt{(x_2 - x_1)^2 + (y_2 - y_1)^2 + (z_2 - z_1)^2} \quad (6)$$

Where (x_1, y_1, z_1) are the coordinates of the maximum dose location in one scan, and (x_2, y_2, z_2) are the coordinates of the same structure's maximum dose location in the subsequent scan, giving the straight-line distance (in mm) between the two points in space[46].

2.8. Statistical Analysis

A paired t-test was performed with an alpha value of 0.05 was used to quantify differences in dose accumulation between the conservative approach and the DIR-based method. A QQ plot was used to evaluate the normality of the dose distributions for both methods, demonstrating that they both followed a normal distribution. Consequently, a paired t-test was appropriate for statistical comparison. One extreme outlier in the small bowel data was identified and eliminated prior to analysis because of its disproportionate influence on variance and deviation from expected clinical values likely due to extreme distortions in the small bowel regions after DIR. The paired t-test was applied to key dose metrics, including D_{2cc} for OARs and D_{90} for the CTV, to determine if significant differences existed between the two methods. Statistical significance was indicated by a p-value threshold of 0.05, with values below this threshold indicating a statistically significant difference.

3. Results

3.1. TRE Analysis for Landmark-Based DIR Accuracy

The spatial accuracy of deformable image registration (DIR) was first assessed in terms of target registration error (TRE), which measures the displacement between corresponding anatomical landmarks after registration. Accurate DIR is particularly important to ensure that dose accumulation across fractions is spatially meaningful.

TRE was computed between HDR fraction 1 and HDR fraction 2 for each patient by using four anatomical landmarks consistently identified in both scans. This fraction pair was chosen to provide an example of typical inter-fraction anatomical displacement in the HDR brachytherapy course of treatment, while minimizing the confounding effects of large anatomical differences that can be seen when comparing EBRT scans with HDR brachytherapy scans.

The pooled box-and-whisker plot in Figure 9 shows TRE distributions across all landmarks for each DIR method. Since all landmarks produced comparable TRE trends, using the pooled landmarks provides a general assessment of registration accuracy. Contour-based DIR had consistently the largest TRE values across all landmarks with a mean TRE of 17.2 mm (95% CI: 12.82-21.51 mm). In contrast, hybrid-based DIR demonstrated the lowest TRE, with a mean of 2.71 mm (95% CI: 1.96-3.45 mm), followed closely by image-based DIR with a mean of 2.86 mm (95% CI: 2.03-3.71 mm).

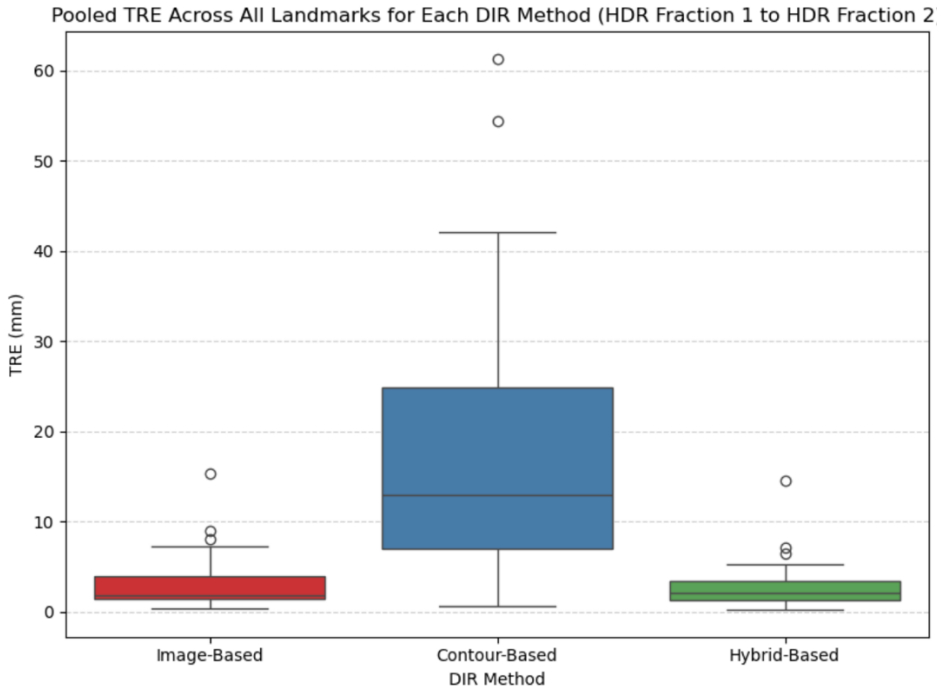

Figure 9 Comparison of target registration error (TRE) in millimeters across different deformable image registration methods, image-based (red), contour-based (blue), and hybrid-based(green), between Fraction 1 and Fraction 2.

3.2. DIR Accuracy

To evaluate the performance of the different types of DIR, the Dice Similarity Coefficient (DSC) and Jaccard Index for each organ across all fraction comparisons were compared. Figures 10 and 11 present box-and-whisker plots summarizing these overlap metrics across all organs for each DIR type (Image-based, Contour-based, Hybrid-based).

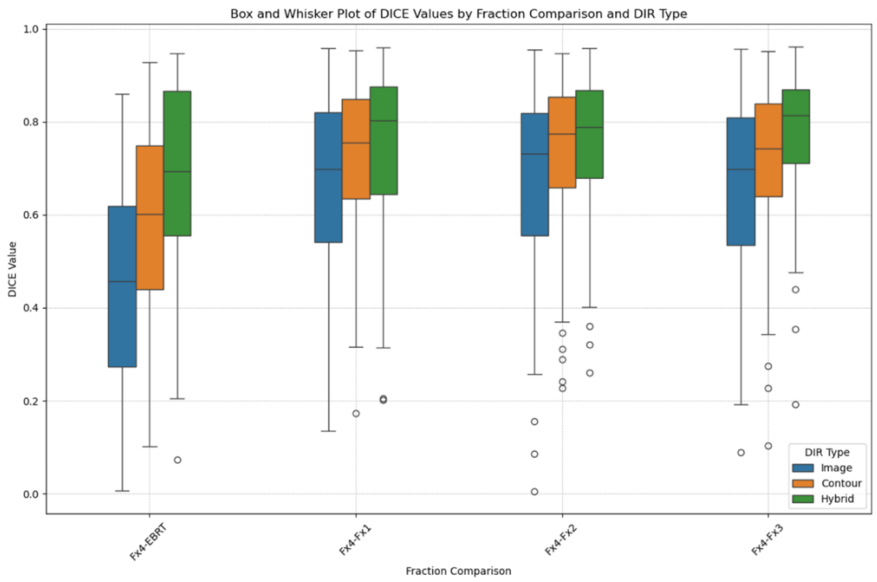

Figure 10 Box-and-whisker plot summarizing the Dice Similarity Coefficient for all contoured organs across different deformable image registration methods, image-based (blue), Contour-based (orange), hybrid-based (green), over all fraction comparisons, illustrating the variability and median DSC values for each method.

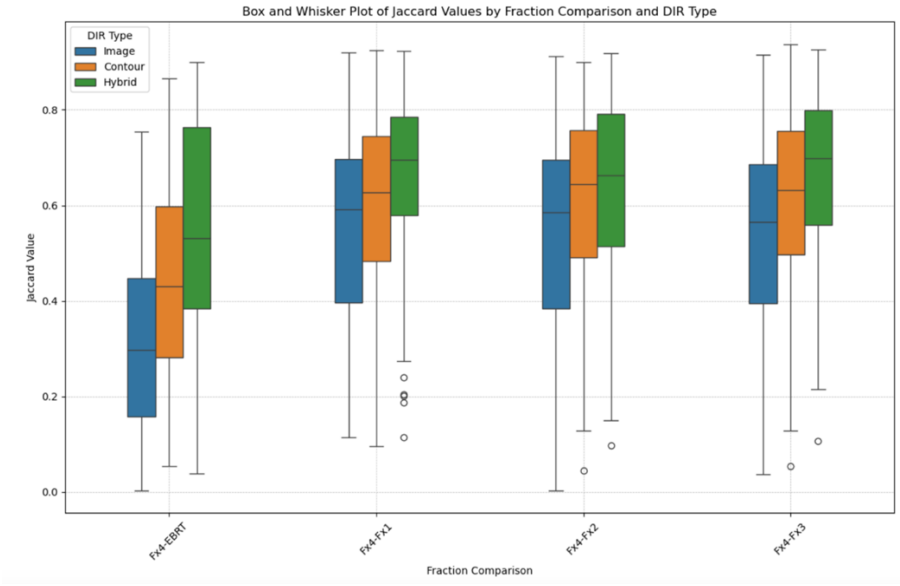

Figure 11 Box-and-whisker plot summarizing the Jaccard Index for all contoured organs across different deformable image registration methods, image-based (blue), Contour-based (orange), hybrid-based (green), over all fraction comparisons, illustrating the variability and median Jaccard Index values for each method.

Overall, the hybrid-based DIR consistently demonstrated the highest DSC values and Jaccard Index values across all fraction comparisons, suggesting there was greatest spatial agreement between deformed and reference structures. The CT_HDRFx4_n -EBRT comparison had the lowest mean DSC with significant spread. Similar observations could be made with respect to the Jaccard Index. To further assess organ performance individually for each comparison, DSC box-and-whisker plots were made for each organ.

The small bowel and sigmoid demonstrated the greatest variability, with lower overall DSC and Jaccard Index values and more variation between DIR methods. The bladder DSC values were consistently higher across all DIR methods, where for all the brachytherapy fractions the bladder DSC was above 0.8, indicating this organ had a more stable contour anatomically and greater spatial overlap between fractions. However, for CT_HDRFx4_n-EBRT comparisons, the mean DSC values were lower compared to other fraction comparisons. Figure 12 summarizes the DSC value comparisons for two representative organs – the bladder as it demonstrated high anatomical stability across fractions, and the small bowel which exhibited greater variability between across fractions.

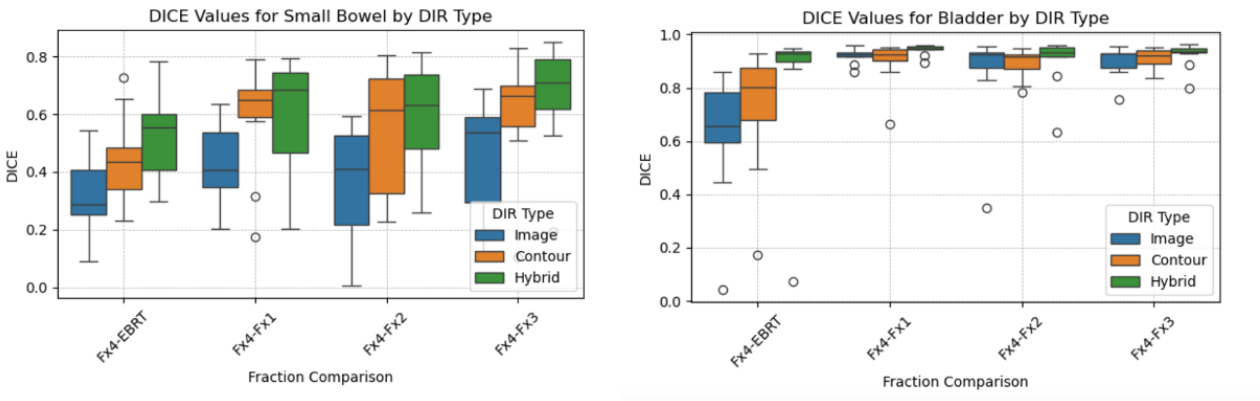

Figure 12 Box-and-whisker plot summarizing the Dice Similarity Coefficient for the bladder (right) and the small bowel (left) across different deformable image registration methods, image-based (blue), Contour-based (orange), hybrid-based (green), over all fraction comparisons, illustrating the variability and median DSC values for each method.

Tables 2 summarizes the mean DSC ± standard deviation (SD) values for the three DIR methods and each fraction comparison. Hybrid-based DIR achieved the highest mean DSC overall, particularly for the HR-CTV, bladder, and rectum, and had lower variability compared to the other two methods. Image-based DIR showed the lowest mean DSC for the sigmoid and small bowel comparisons, with higher variability between fractions indicating the challenges in accurately deforming these regions.

Table 2 Mean DSC +/- SD for each DIR method across all fraction comparisons for each OAR and region of interest.

Mean Dice Similarity Coefficient (±SD) for Image-Based DIR, Contour-only DIR, and Hybrid-Based DIR				
Image-Based DIR	Fx4-EBRT	Fx4-Fx1	Fx4-Fx2	Fx4-Fx3
HR-CTV		0.69 ± 0.11	0.75 ± 0.09	0.68 ± 0.11
Bladder	0.62 ± 0.23	0.92 ± 0.03	0.86 ± 0.18	0.90 ± 0.06
Rectum	0.57 ± 0.16	0.73 ± 0.11	0.73 ± 0.10	0.68 ± 0.16
Sigmoid	0.36 ± 0.17	0.50 ± 0.22	0.52 ± 0.16	0.52 ± 0.19
Small Bowel	0.30 ± 0.14	0.42 ± 0.14	0.36 ± 0.21	0.45 ± 0.20
Applicator		0.70 ± 0.15	0.77 ± 0.07	0.74 ± 0.11
Contour-only DIR	Fx4-EBRT	Fx4-Fx1	Fx4-Fx2	Fx4-Fx3
HR-CTV		0.75 ± 0.17	0.80 ± 0.06	0.80 ± 0.10
Bladder	0.78 ± 0.23	0.90 ± 0.09	0.89 ± 0.06	0.91 ± 0.04
Rectum	0.67 ± 0.10	0.79 ± 0.09	0.79 ± 0.10	0.73 ± 0.12
Sigmoid	0.57 ± 0.23	0.65 ± 0.16	0.62 ± 0.21	0.59 ± 0.24
Small Bowel	0.48 ± 0.13	0.59 ± 0.19	0.54 ± 0.23	0.60 ± 0.20
Applicator		0.66 ± 0.11	0.64 ± 0.14	0.69 ± 0.11
Hybrid-Based DIR	Fx4-EBRT	Fx4-Fx1	Fx4-Fx2	Fx4-Fx3
HR-CTV		0.78 ± 0.13	0.81 ± 0.08	0.82 ± 0.08
Bladder	0.84 ± 0.27	0.94 ± 0.02	0.90 ± 0.10	0.92 ± 0.05
Rectum	0.78 ± 0.07	0.79 ± 0.10	0.81 ± 0.08	0.79 ± 0.10
Sigmoid	0.57 ± 0.20	0.59 ± 0.22	0.62 ± 0.15	0.64 ± 0.17
Small Bowel	0.51 ± 0.17	0.60 ± 0.21	0.59 ± 0.19	0.67 ± 0.19
Applicator		0.78 ± 0.08	0.77 ± 0.07	0.79 ± 0.06

3.3. Inter-fraction Shifts in Maximum Dose Location

To examine the effects of anatomical variability on DIR performance even further, the spatial movement of the maximum dose location was evaluated for each organ across adjacent CT scans. The Euclidean distance between the coordinates of the maximum dose voxel for each structure was calculated from one fraction to the next. The distance values for each structure are depicted in Figure 13 as a bar chart, with individual bars representing each structure and value labels indicating the specific movement magnitude in millimeters. The greatest spatial shifts were observed between the EBRT scan and the first fraction of HDR brachytherapy. Specifically, the maximum dose location moved 116.8 mm for the bladder, 77.8 mm for the HR-CTV, and 72.4 mm

for the sigmoid. These values were substantially higher than those calculated between the subsequent fractions of HDR brachytherapy.

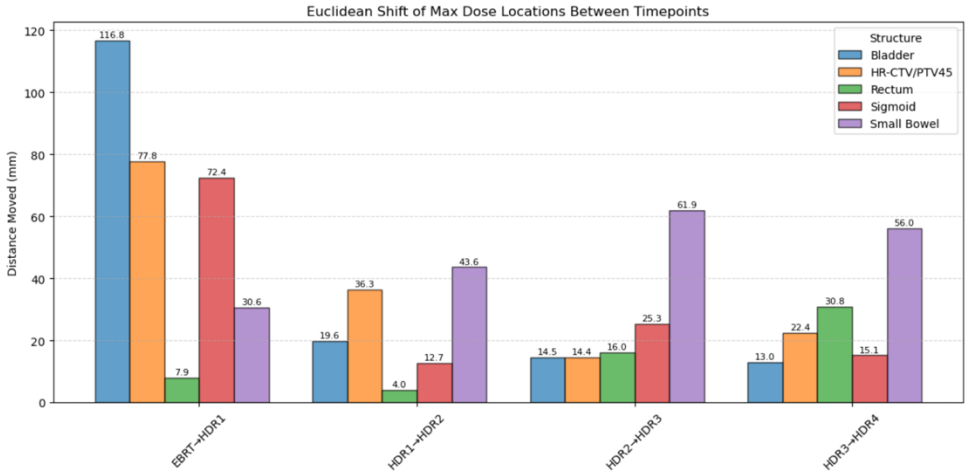

Figure 13 Bar chart showing the magnitude of movement (in mm) of maximum dose location for each structure between adjacent CT scans. Distances were calculated using Euclidean distance between coordinates, with individual bars representing each organ. Value labels above the bars indicate the specific distance moved for each time interval.

3.4. Dose Comparison

To evaluate the dosimetric impact of deformable image registration by computing and combining EQD_2 doses using both the conservative summation method, which assumes consistent spatial location of maximum dose regions for each treatment session, and the DIR-based deformation approach. The hybrid-based DIR was selected for dose accumulation as it had demonstrated the lowest TRE and the highest overlap accuracy among the DIR algorithms for all organs of interest. Hybrid-based DIR consistently achieved the highest DSC values with the least variability across cases, supporting its selection as the most reliable method for cumulative dose estimation.

Figure 14 presents pre- and post-deformation dose values for each structure, showing the general dose changes associated with dose accumulation based on DIR. The plots show a comparison of dose distributions obtained from the conservative and DIR-based dose accumulation methods, illustrating the impact on dose delivery to both the HR-CTV and OARs from the pre- and post-deformation comparisons. It helps to understand the clinical impact of cumulative dose variations to critical structures and treatment targets caused by anatomical changes and deformation during HDR brachytherapy combined with EBRT.

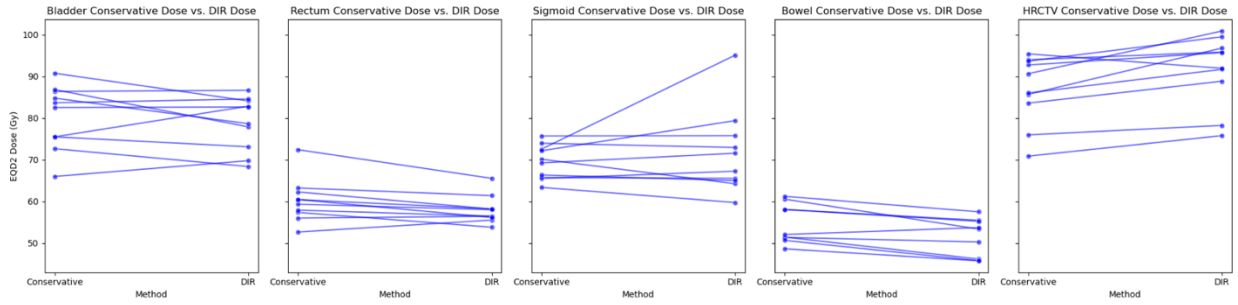

Figure 14 Pre-post EQD_2 dose difference plots comparing the conservative dose accumulation methods. Dose metrics shown are D_{2cc} for OARs (bladder, rectum, sigmoid, and small bowel) and D_{90} for the high-risk clinical target volume (HR-CTV), presented left to right.

Statistical analysis revealed significant differences in dose accumulation between conservative and DIR-based approaches for the small bowel (p=0.0054), the rectum (p=0.0279) and HR-CTV (p=0.0065). The small bowel demonstrated a mean decrease of 3.20 Gy EQD_2 in D_{2cc}, while the rectum also experienced a mean reduction in D_{2cc} of 2.24 Gy EQD_2. The HR-CTV showed an increase of accumulated D_{90} with a mean of 4.67 Gy EQD_2. The mean dose difference 95% confidence interval excludes zero, indicating that the observed difference is unlikely due to

random variation. All other organ doses were found to be statistically insignificant ($p>0.05$), as reported in Table 3.

Table 3 Mean Dose differences for OARs and HR-CTV in Gy EQD_2 and Mean percent differences between the conservative summing of doses and the DIR dose accumulation method, including the 95% confidence interval.

Mean Dose Differences and 95% Confidence Intervals for Each Organ and HR-CTV

	Mean Dose Difference	95% Confidence Interval	Mean % Difference
Bladder	-1.59	(-5.20, 2.02)	-1.68%
Rectum	-2.24	(-4.17, -0.30)	-0.03%
Sigmoid	2.18	(-3.52, 7.89)	2.94%
Bowel	-3.2	(-5.15, -1.24)	-5.78%
HR-CTV	4.67	(1.67, 7.67)	5.49%

For three patients identified to have a steep increase in HR-CTV dose following DIR, Reg Refine® was selectively applied to improve local deformation accuracy. Without the application of Reg Refine®, the mean difference in cumulative HR-CTV D_{90} using the DIR dose accumulation method compared to the conservative method was 4.67 Gy EQD_2 (95% CI: 1.67, 7.67). Upon the application of Reg Refine®, the mean cumulative D_{90} was 4.17 Gy EQD_2 (95% CI: 1.28, 7.06), resulting in a slight reduction in the observed dose.

4. Discussion

Overall, study findings suggest that DIR-based dose accumulation provided lower organ dose estimations compared to the conservative dose summation method which is currently standard practice. The organs that demonstrated a statistically significant D_{2cc} difference between the methods were the small bowel and the rectum. Additionally, a significant increase in cumulative D_{90} was observed for the HR-CTV utilizing the DIR-based accumulation method. The bladder and sigmoid did not report statistically significant differences to warrant any mention. This may suggest that, for some organs, DIR-based accumulation does not substantially alter dose evaluation compared to conservative methods. However, without definitive validation of registration accuracy, particularly in areas with minimal motion or less complex anatomy, it remains unclear whether these differences reflect true clinical advantage. However, for structures like the small bowel and the rectum, dose estimation is challenging due to excessive motion and deformation, and DIR may be more reliable in estimating the accumulated dose.

4.1. Superior DIR Algorithm

Among the different DIR algorithms evaluated, the hybrid-based DIR provided the most accurate registration between images, which was not unexpected. Hybrid-based DIR uses both intensity-based and contour-based information from a CT scan, allowing it to more effectively correct for anatomical deformations than with intensity- or contour-based approaches alone. Given that this study involved multiple CT scans obtained over the course of EBRT and HDR brachytherapy, there would be a reasonable probability for the hybrid-based DIR to be superior as it recognizes features of both the image intensities and predefined anatomical structures. The

ability to combine these two forms of information, minimized large misalignments that can occur when relying on intensity or contour information alone, likely providing a more stable and accurate registration outcome. Importantly, the standard deviations and 95% confidence intervals (CIs) for the TRE values revealed that the hybrid-based DIR method had the smallest TRE variability, suggesting it offers more reliable and consistent results across patients and fractions. The consistency and reproducibility could be primarily driven the hybrid-based method's ability to minimize the complications and inherent unpredictability of complex anatomical changes between treatment fractions, especially in high dose regions.

The contour-based DIR method demonstrated higher TRE values compared to the other algorithms, and pooled landmark analyses suggested TREs reaching up to roughly 42.5 mm. The standard deviation analyses suggested greater uncertainty in the contour-based DIR method, which could indicate that large misalignments were not simply random isolated events but distributed more broadly across different anatomical regions. However, the DSC for contour-based DIR was often better than image-based DIR despite the large TRE values. The mentioned contradiction can be justified by the fundamental differences in how these metrics evaluate registration accuracy. Contour-based DIR assesses the accuracy of the registration by managing the alignment of the organ contours through registration. The algorithms improved DSC could mean that the deformed contours are correctly matched; however, the method does not utilize image intensity information, meaning there is no guarantee that the internal anatomical structures align accurately, which would lead to increased uncertainty in the point-based dose mapping. Contour-based DIR prioritizes external contour matching, which can lead to internal misalignments that are not reflected in the DSC metric but are captured in the TRE calculations. This suggests that contour-based DIR may

perform well to identify large approximations of organ shapes, but it may introduce distortions or misalignment of internal structures that mislead the accuracy of point-based dose mapping, particularly for organs of highly movable nature. As mentioned before, image-based DIR uses voxel intensity information rather than predefined structures, which offer better TRE values encapsulating internal anatomical landmarks more accurately, even if the organ contours do not overlap as precisely. The hybrid-based DIR method, was likely superior to the two approaches by leveraging information from both algorithms, achieving a more consistent and likely anatomically correct registration.

4.2. Dose Differences

The significant dose difference in D_{2cc} observed in the small bowel comparing conservative and DIR-based methods – 3.20 Gy EQD_2 – is an important reminder of the anatomical motion to consider when evaluating cumulative dose. The small bowel itself is inherently more variable than many other organs due to its peristaltic motion, gradual changing filling status, and degree of elasticity and flexibility. Given these inherent characteristics, significant differences in positional and shape variability exist between treatment fractions, meaning it would be unreliable to use rigid summation-based methods to sum dose in the small bowel. While the bladder can change volume but will generally stays in a stable position, and the rectum is partially constrained by pelvic anatomy, the small bowel has no such constraints and may experience substantial motion and deformation. The variability of the small bowel is important because conservative summation methods would not account for anatomical changes and inter-fraction motion adequately, making it especially problematic regarding dose miscalculations.

To further examine the variability, Euclidean distances were calculated between the coordinates of maximum dose locations for each structure in adjacent scans. As discussed in the results, the maximum dose location shifts were greatest between the EBRT and the HDR fraction 1 scans, reiterating fundamental differences in spatial maximum dose positioning of these types of fractionations. Among all the structures analyzed, the small bowel exhibited the greatest shifts in maximum dose location, with shifts up to 61.9 mm, between adjacent HDR brachytherapy fractions. The high variability in maximum dose location was useful in accentuating the benefits of DIR, as conservative methods would not capture such large displacements in mobile structures, because these approaches treat maximum dose regions as fixed anatomical positions. It is perhaps the small bowel's motion that provides the rationale of being one of the organs to exhibit a statistically significant difference in dose in the analysis performed following the DIR-based dose accumulation.

Although less pronounced than in the small bowel, the rectum demonstrated a statistically significant mean decrease of 2.24 Gy in D_{2cc}, between conservative and DIR-based dose estimates as well. This difference is likely due to the rectum's distinct anatomical and physiological properties. Even though the rectum is partially constrained by pelvic anatomy, it is a hollow organ that undergoes dynamic volume and shape changes due to variable gas and stool content. These changes can lead to deformation and positional shifts, noticeable across all treatment fractions. Additionally, rectal filling protocols are usually less consistent than for the bladder, for example, further contributing to inter-fraction variability. Because conservative dose summation methods do not account for these shape or positional changes, they may inaccurately assume spatial overlap of high-dose regions across fractions. Contrary to DIR-based accumulation which attempts to

account for these deformations, allowing a more anatomically accurate estimate of true accumulated dose to the rectum. This supports the use of DIR-dose estimation in rectal dose evaluations when inter-fraction motion seems to be pronounced or when doses approach toxicity thresholds.

Interestingly, Figure 14 shows that in several cases, DIR-based dose accumulation resulted in higher doses to organs at risk than the conservative method. At first glance, this seems counterintuitive since conservative dose summation assumes that the high-dose regions from each fraction spatially overlap, functioning as a worst-case scenario for cumulative exposure. The observation that DIR-based estimates sometimes exceed those of the conservative method suggests that deformation-based warping may be introducing artificial dose accumulation. This could stem from inaccuracies in aligning either the anatomical structures or the dose distributions across fractions. These effects are likely most pronounced in regions with steep dose gradients, such as areas surrounding HDR applicators, where even small misregistration can lead to disproportionately high estimated doses. This reinforces the importance of carefully validating DIR performance, particularly when dose estimations are being used to make clinical judgements regarding potential toxicity. While DIR offers a more anatomically informed approach, it may still introduce distortions that need to be accounted for during interpretations.

Following DIR-based dose estimation, the HR-CTV was the only structure that demonstrated a significant increase in cumulative dose. This is likely a result of the better alignment of anatomy concerning the high-dose areas from HDR brachytherapy across fractions. Due to patient anatomy, the applicator placement may vary in terms of angle, depth, and

positioning, from fraction to fraction, which can lead to spatial shifts in the location of the maximum doses. Conservative summation methods assume perfect overlap of dose distributions in a fixed coordinate space, and this often underrepresents dose accumulation in regions where high-dose volumes do not align precisely across fractions. Addressing the inter-fraction anatomical variability and improving alignment precision of HR-CTV contours across fractions aids in depicting the spatially delivered dose more realistically. Such improvements in alignment are particularly important for HDR brachytherapy where steep gradients in dose distributions, which make local dose estimations extremely sensitive to small shifts. The increase in HR-CTV dose through DIR indicates that the potential advantage in using deformable techniques may lie in how accurately they assess target coverage.

The high degree of uncertainty in DIR for mobile structures was evident in the variability of TRE, DSC, and Jaccard Index metrics. The standard deviations and 95% CIs demonstrated greater uncertainty for the small bowel and rectum registration, and the DSC and Jaccard scores exhibited wider CIs in comparison to the more stable organs, such as the bladder. The wider CIs for these metrics in the Image-based and Contour-based methods are suggestive of variable accuracy of the DIR of organs that experience higher motion. On the other hand, the hybrid-based DIR method, for both the small bowel and rectum, showed smaller CIs, which reflect higher reliability of accurately registering these organs despite having a high degree of motion and shape change related uncertainty. These findings support using hybrid methods when dealing with highly deformable and compositionally heterogeneous structures like the rectum and the small bowel, where things like gas, fluid, and fecal content, affect CT image intensity, making image-based DIR alone less effective in achieving accurate registration. Using a combination of contour-based and

intensity-information through a hybrid-based DIR mitigates some of those challenges and improves the accuracy of the dose mapping.

It is crucial to determine whether these variations are clinically significant despite the fact there is a significant difference in small bowel and rectal dose between methods. The conservatively summed small bowel doses in this study did not reach concerning levels (e.g., 70 Gy EQD_2), which begs the question of whether using DIR-based dose accumulation would yield enough clinical benefit to warrant the additional complexity. DIR may not be as necessary if the conservative method already provides a dose estimate that remains below known toxicity thresholds. However, when small bowel dose is a clinical concern, as in the cases of patients receiving higher EBRT doses or those with predisposing gastrointestinal conditions, DIR-based dose accumulation may provide a more accurate assessment of toxicity risk by giving a more precise representation of the true dose received by the small bowel. Similarly, rectal doses appeared lower using the conservative method. However, in clinical practice, brachytherapy plans are often limited by rectal dose constraints, and many patients do not reach the target $D_{90} > 90$ Gy EQD_2 for HR-CTV due to OAR tolerances. In these cases, DIR may provide added value by more accurately capturing rectal dose near the threshold.

For the HR-CTV, there is a concern for treatment effectiveness, rather than toxicity. The DIR-based approach provided a higher estimated cumulative dose, likely because of improved alignment of high-dose regions across HDR brachytherapy fractions. This might indicate a more realistic representation of the therapeutic dose that was delivered to the target. In situations where

dose escalation or precise target coverage is a priority, DIR may facilitate better informed clinical decision-making.

Another important consideration is the uncertainty generated by the DIR process itself. Variability in registration accuracy is indicated by the spread in TRE, DSC, and Jaccard Index values. This variation extends into the dose accumulation process and could affect the reliability of the final summed doses. If the uncertainty surrounding DIR-based accumulation is substantial compared to the magnitude of the dose differences being considered, the clinical utility of these techniques may be limited. Additionally, Zhong et al.[47] note that the uncertainties associated with deformable image registration must be considered when interpreting accumulated dose distributions. The accuracy of dose mapping may be impacted by residual uncertainties even when DIR enhances anatomical alignment. When interpreting DIR-based cumulative doses, it is crucial to take into consideration both the observed dose difference magnitude and the inherent uncertainty introduced by performing deformable image registration in order to ensure that dose assessments accurately reflect patient risk.

To better understand how spatial misalignments might affect dose accumulation, TRE values were quantified at anatomically relevant locations near the applicator. A landmark was placed 2.16 cm from the edge of the ovoid, at the bladder catheter entrance, which is a site close to multiple organs at risk. After performing hybrid-based DIR and point-based alignment using bony anatomy, the TRE at this location was measured to be approximately 2.98 mm.

To estimate how this spatial uncertainty might translate to dosimetric uncertainty, the dose falloff was approximated using the distance between isodose lines. The distance from the 100% to the 50% isodose line was measured to be 0.34 cm, and the 50% to 10% was 1.74 cm. Based on this steep dose gradient, an estimated 6.85% dose uncertainty was associated with the 2.98 mm TRE at this point. A second landmark placed 4.31 cm from the applicator ovoid edge, yielded a TRE of 0.999 mm, resulting in an estimated dose uncertainty of 2.3%. These findings suggest that registration uncertainty and its impact on dose estimation are greatest near the applicator, where the dose gradient is steepest, and decrease with increasing distance. This spatial relationship between TRE and dosimetric uncertainty highlights the importance of carefully evaluating alignment accuracy in high-dose regions, as small geometric discrepancies can lead to clinically meaningful differences in accumulated dose estimates.

While lower DIR-based dose estimates for OARs may seem favorable, this interpretation relies on the assumption that the registration is accurate. If the DIR process underestimates the dose due to registration inaccuracies, especially in high-dose gradient regions or highly deformable structures, there is a risk that the actual dose delivered to an organ is higher than what is reported. This risk of underestimation is important to consider, as lower reported dose values are only clinically meaningful if they accurately reflect the true anatomical and dosimetric reality. Therefore, although DIR offers advantages in accounting for anatomical variability, its limitations and potential for under-reporting dose should also be taken into account when interpreting results.

These findings demonstrate that both conservative and DIR-based dose accumulation methods have limitations that are context dependent. While the conservative approach may fail to

account for anatomical variability, especially in mobile structures, DIR introduces its own set of uncertainties, particularly in regions with steep dose gradients where even small misregistrations can lead to large discrepancies in estimated dose. As such, determining the most appropriate method depends on the clinical scenario, including the degree of anatomical motion, proximity to high-dose regions, and the required accuracy of dose estimation. Understanding the nature and limitations of each approach is essential for interpreting cumulative dose distributions and making informed clinical decisions.

4.3. Dose-Toxicity Threshold Considerations

If DIR-based dose accumulation results in notable differences compared to conventional summation, there may be implications for established dose-toxicity relationships. The EMBRACE II protocol, for example, derived its dose constraints and toxicity thresholds using conventional methods that do not account for anatomical deformation or inter-fraction motion. If DIR approaches produce higher or lower accumulated doses to certain organs, particularly in mobile structures like the bowel, these thresholds may no longer reflect true clinical risk. This raises the possibility that some dose-toxicity relationships may need to be re-evaluated if DIR becomes a standard part of dose summation.

4.4. Comparison to Prior Studies

Previous studies on DIR-based dose accumulation in gynecologic radiotherapy have given the bladder and the rectum more attention that the small bowel. Mohammadi et al.[27], for example, employed hybrid-based DIR to identify notable variations between accumulated bladder and rectal

doses; yet their study ignored inter-fraction motion. Abe et al.[48] found no significant differences between DIR-based and conservative summation techniques; however, they did not identify the DIR algorithm that was employed, making a direct comparison more difficult. Zhao et al.[33] also assessed cumulative dose distributions in patients with cervical cancer using deformable image registration, but their analysis was restricted to the bladder and rectum and did not account for small bowel doses. Additionally, they utilized the Varian Velocity software without specifying which the DIR algorithm was used, further limiting direct comparability to this study.

The dose variations seen in the small bowel and rectum are potentially due to the impact of inter-fraction motion which impacts the accuracy of cumulative dose calculations. This study highlights the importance of considering highly mobile structures for dose evaluation, especially for patients receiving higher doses or exhibiting greater anatomical variability, while previous studies have mostly concentrated on the bladder and rectum without comparing different DIR algorithms.

These findings also raise important considerations for how DIR-based dose accumulation could be incorporated into clinical workflows. In this analysis, doses were registered to the final brachytherapy fraction (CT_HDRFx4_n), allowing for retrospective evaluation of cumulative dose. However, for DIR-based dose accumulation to be useful prospectively, such as during treatment planning or adaptation, registration would need to be performed to an earlier fraction, such as the first HDR fraction. Aligning to HDR fraction 1 would allow the cumulative dose information from prior fractions to inform decisions during ongoing treatment, potentially guiding

plan adaptation or dose constraints in real time. This shift in reference frame would be necessary for DIR-based dose accumulation to meaningfully contribute to planning workflows.

4.5. Limitations

This study has several limitations worth mentioning with the first being that the statistical power might have been affected by the small sample size. Additionally, the presence of the applicator, which adds to the challenges in deformable image registration, resulted in a lower overall DIR accuracy when aligning EBRT and HDR brachytherapy images, even though hybrid-based DIR was found to provide the most accurate registrations. Further research might examine improved registration methods designed especially for situations involving brachytherapy applicators.

Another limitation was that visual inspection was the main method used to evaluate DIR accuracy, which might not be enough to identify subtle misalignments. The entire cohort did not use tools like Reg Refine® and Reg Reveal® consistently, but they were tested on a subset of patients and demonstrated improvements in local deformation accuracy, which slightly moderated the cumulative dose difference highlighting its value in refining dose mapping in critical regions. Although the time-consuming nature of these tools and the possibility of user variability restrict their wider application, their selective use demonstrates the benefit of localized refinement, particularly for targets like the HR-CTV where accurate alignment influences perceived dose coverage. To increase reproducibility, future research should concentrate on creating uniform standards for when and how to apply refinement tools.

Lastly, inter-observer variability in contouring was not assessed in this study even though it may have a substantial impact on dose accumulation outcomes. Additional uncertainties that could spread throughout the DIR process can be introduced by variations in target and OAR delineation among physicians. The effect of contouring variations on cumulative dose summations should be evaluated in future research.

5. Conclusion

This study assessed the accuracy and clinical relevance of DIR-based cumulative dose estimation in gynecological HDR brachytherapy. Achieving the best DSC values and lower TREs, hybrid-based DIR outperformed image-based and contour-based techniques in registration performance. Compared to the standard conservative summation techniques, DIR-based dose accumulation regularly produced marginally lower projected doses for the bladder, rectum, and small bowel. The small bowel and rectum showed a statistically significant difference in cumulative D_{2cc}, likely due to its inherent inter-fraction mobility. Additionally, the HR-CTV demonstrated a statistically significant increase in D_{2cc} due to improved alignment of high-dose regions with DIR.

The results underline the importance of accounting for anatomical variability, particularly in mobile structures like the small bowel and rectum, when calculating cumulative dose. In these situations, conservative summation techniques assuming fixed anatomical position may overstate the real anatomical dose. Although, DIR-based summation might not provide a significant clinical benefit over conventional methods for more stable structures like the bladder.

The DIR process itself introduces registration uncertainty that propagates into final dose distributions. Variability in DIR accuracy, as shown through TRE, DSC, and Jaccard Index measures, influences the reliability of accumulated dose estimates. Thus, a thorough analysis of DIR performance is necessary to guarantee that dose evaluations are indicative of actual anatomical state.

To further increase registration accuracy and reproducibility, future work should concentrate on standardizing localized refinement tools like Reg Refine®. Validation efforts can be strengthened by inter-observer variability analyses and larger patient cohorts.

Overall, this study supports the potential of DIR-based dose accumulation to improve dose evaluation in mobile organs during gynecological HDR brachytherapy, but it also emphasizes the necessity of thoughtful implementation, consistent validation, and careful integration into clinical practice.

Appendix

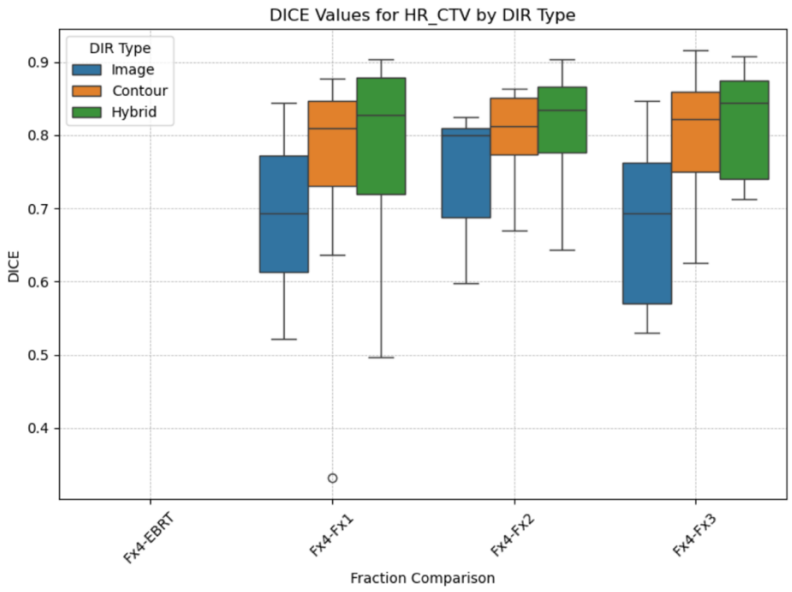

Figure 15 Box-and-whisker plot summarizing the Dice Similarity Coefficient for the HR-CTV across different deformable image registration methods, image-based (blue), Contour-based (orange), hybrid-based (green), over all fraction comparisons, illustrating the variability and median DSC values for each method.

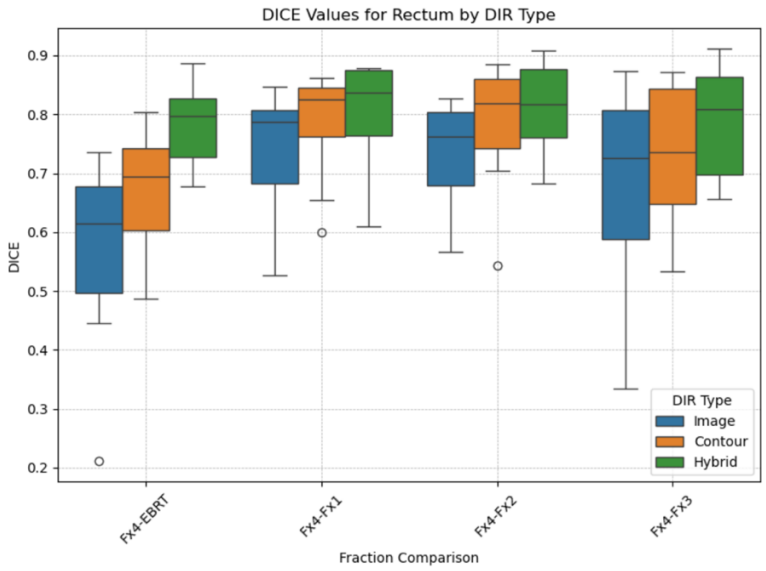

Figure 16 Box-and-whisker plot summarizing the Dice Similarity Coefficient for the Rectum across different deformable image registration methods, image-based (blue), Contour-based (orange), hybrid-based (green), over all fraction comparisons, illustrating the variability and median DSC values for each method.

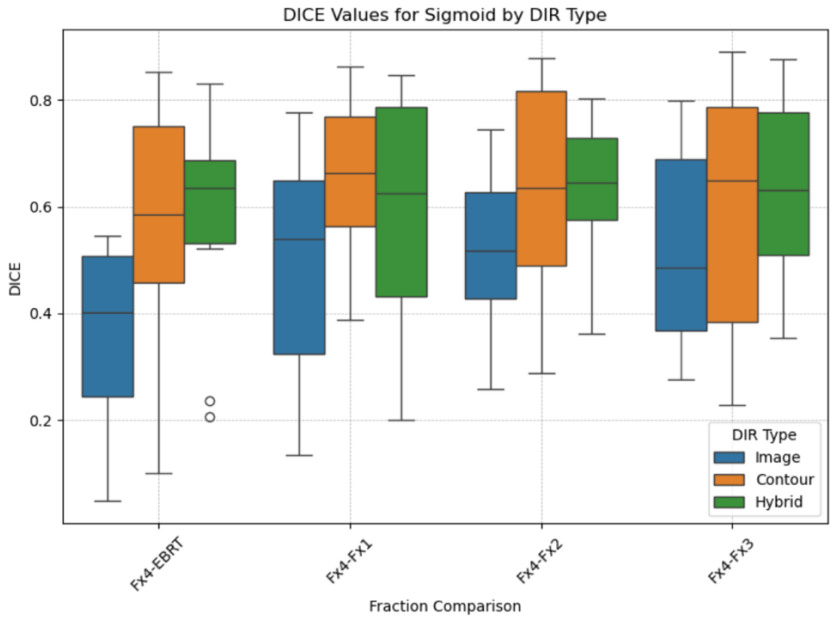

Figure 17 Box-and-whisker plot summarizing the Dice Similarity Coefficient for the Sigmoid across different deformable image registration methods, image-based (blue), Contour-based (orange), hybrid-based (green), over all fraction comparisons, illustrating the variability and median DSC values for each method.

References

1. MIM Software. Published online 2024.

2. Weiner AA, Schwarz JK. Intracavitary Brachytherapy for Gynecologic Malignancies: Applications and Innovations. *Mo Med*. 2015;112(5):366-372.

3. Scanderbeg DJ, Yashar C, Ouhib Z, Jhingran A, Einck J. Development, implementation, and associated challenges of a new HDR brachytherapy program. *Brachytherapy*. 2020;19(6):874-880. doi:10.1016/j.brachy.2020.08.018

4. Han K, Milosevic M, Fyles A, Pintilie M, Viswanathan AN. Trends in the Utilization of Brachytherapy in Cervical Cancer in the United States. *Int J Radiat Oncol Biol Phys*. 2013;87(1):111-119. doi:10.1016/j.ijrobp.2013.05.033

5. Tanderup K, Eifel PJ, Yashar CM, Pötter R, Grigsby PW. Curative Radiation Therapy for Locally Advanced Cervical Cancer: Brachytherapy Is NOT Optional. *Int J Radiat Oncol Biol Phys*. 2014;88(3):537-539. doi:10.1016/j.ijrobp.2013.11.011

6. Shrivastava SK, Mahantshetty U, Narayan K. Principles of radiation therapy in low-resource and well-developed settings, with particular reference to cervical cancer. *Int J Gynecol Obstet*. 2015;131(S2):S153-S158. doi:10.1016/j.ijgo.2015.06.013

7. Cheung ESN, Wu PY. Current Paradigm and Future Directions in the Management of Nodal Disease in Locally Advanced Cervical Cancer. *Cancers*. 2025;17(2):202. doi:10.3390/cancers17020202

8. Nath R, Anderson LL, Luxton G, Weaver KA, Williamson JF, Meigooni AS. Dosimetry of interstitial brachytherapy sources: recommendations of the AAPM Radiation Therapy Committee Task Group No. 43. American Association of Physicists in Medicine. *Med Phys*. 1995;22(2):209-234. doi:10.1118/1.597458

9. Gibbons JP, Khan F. Low-Dose-Rate Brachytherapy: Rules of Implantation And Dose Specifications. In: *Khan's The Physics of Radiation Therapy*. Six. Wolters Kluwer; 2014:604-676.

10. Jayakody M, Jeyasugiththan J, Rajasooriyar C, Chougule A. Dosimetry procedure to verify dose in High Dose Rate (HDR) brachytherapy treatment of cancer patients: A systematic review. *Phys Med*. 2022;96:70-80. doi:10.1016/j.ejmp.2022.02.022

11. Strohmaier S, Zwierzchowski G. Comparison of 60Co and 192Ir sources in HDR brachytherapy. *J Contemp Brachytherapy*. 2011;3(4):199-208. doi:10.5114/jcb.2011.26471

12. High Dose Rate Brachytherapy | Oncology Medical Physics. Accessed March 10, 2025. https://oncologymedicalphysics.com/high-dose-rate-brachytherapy/

13. Wilkinson D. High dose rate (HDR) brachytherapy quality assurance: a practical guide. *Biomed Imaging Interv J*. 2006;2(2):e34. doi:10.2349/biij.2.2.e34

14. Geneva | Brachytherapy | Gynecological Applicator | Elekta. Accessed March 10, 2025. https://www.elekta.com/products/brachytherapy/geneva/

15. Venezia | Brachytherapy | Gynecological Applicator | Elekta. Accessed March 10, 2025. https://www.elekta.com/products/brachytherapy/venezia/

16. Hsu ICJ, Speight J, Hai J, Vigneault E, Phillips T, Pouliot J. A comparison between tandem and ovoids and interstitial gynecologic template brachytherapy dosimetry using a hypothetical computer model. *Int J Radiat Oncol Biol Phys*. 2002;52(2):538-543. doi:10.1016/S0360-3016(01)02691-8

17. Albuquerque K, Hrycushko BA, Harkenrider MM, et al. Compendium of fractionation choices for gynecologic HDR brachytherapy—An American Brachytherapy Society Task Group Report. *Brachytherapy*. 2019;18(4):429-436. doi:10.1016/j.brachy.2019.02.008

18. van Leeuwen CM, Oei AL, Crezee J, et al. The alfa and beta of tumours: a review of parameters of the linear-quadratic model, derived from clinical radiotherapy studies. *Radiat Oncol*. 2018;13(1):96. doi:10.1186/s13014-018-1040-z

19. Horwitz TS Eric M. Hypofractionated Radiotherapy for Localized Prostate Cancer: A New Standard of Care? Accessed April 18, 2025. https://ascopost.com/issues/september-10-2016/hypofractionated-radiotherapy-for-localized-prostate-cancer-a-new-standard-of-care/

20. Fowler JF. The radiobiology of prostate cancer including new aspects of fractionated radiotherapy. *2005/05/01*. 44(3):265-276. doi:10.1080/02841860410002824

21. Romano KD, Hill C, Trifiletti DM, et al. High dose-rate tandem and ovoid brachytherapy in cervical cancer: dosimetric predictors of adverse events. *Radiat Oncol Lond Engl*. 2018;13:129. doi:10.1186/s13014-018-1074-2

22. Tanderup K, Poetter R, Lindegaard J, et al. *EMBRACE II Study Protocol*. EMBRACE Consorium; 2016. Accessed March 26, 2025. https://www.embracestudy.dk/Public/Default.aspx?main=2&sub=16&embrace=embrace2

23. Viswanathan AN, Lee LJ, Eswara JR, et al. Complications of pelvic radiation in patients treated for gynecologic malignancies. *Cancer*. 2014;120(24):3870-3883. doi:10.1002/cncr.28849

24. Oh S, Kim S. Deformable image registration in radiation therapy. *Radiat Oncol J*. 2017;35(2):101-111. doi:10.3857/roj.2017.00325

25. Piper J, Nelson A, Harper J. *Deformable Image Registration in MIM Maestro: Evaluation and Description*. MIM Software Inc.; 2013. https://www.mimsoftware.com/literature/publications

26. Motegi K, Tachibana H, Motegi A, Hotta K, Baba H, Akimoto T. Usefulness of hybrid deformable image registration algorithms in prostate radiation therapy. *J Appl Clin Med Phys*. 2018;20(1):229-236. doi:10.1002/acm2.12515

27. Mohammadi R, Mahdavi SR, Jaberi R, et al. Evaluation of deformable image registration algorithm for determination of accumulated dose for brachytherapy of cervical cancer patients. *J Contemp Brachytherapy*. 2019;11(5):469-478. doi:10.5114/jcb.2019.88762

28. Piper J, Nelson A, Harper J. *VoxAlignTM Deformable Engine White Paper*. MIM Software Inc.; 2018.

29. Kubota Y, Okamoto M, Li Y, et al. Evaluation of Intensity- and Contour-Based Deformable Image Registration Accuracy in Pancreatic Cancer Patients. *Cancers*. 2019;11(10):1447. doi:10.3390/cancers11101447

30. MIM Software Inc. *MIM Software User Guide*. MIM Software Inc.; 2023. www.mimsoftware.com

31. Swamidas J, Kirisits C, Brabandere MD, Hellebust TP, Siebert FA, Tanderup K. Image registration, contour propagation and dose accumulation of external beam and brachytherapy in gynecological radiotherapy. *Radiother Oncol*. 2020;143:1-11. doi:10.1016/j.radonc.2019.08.023

32. GEC-ESTRO Committee. Accessed May 22, 2025. https://www.estro.org/About/ESTRO-Organisation-Structure/Committees/GEC-ESTRO-Committee

33. Zhao T, Chen Y, Qiu B, et al. Evaluating the accumulated dose distribution of organs at risk in combined radiotherapy for cervical carcinoma based on deformable image registration. *Brachytherapy*. 2023;22(2):174-180. doi:10.1016/j.brachy.2022.09.001

34. Millar LPB, Teo BK, Lin LL. Using Deformable Image Registration to Assess the Accuracy of Cumulative External Beam and Intracavitary Brachytherapy ICRU Point Doses in Cervical Cancer. *Int J Radiat Oncol Biol Phys*. 2010;78(3):S411-S412. doi:10.1016/j.ijrobp.2010.07.969

35. Geneva | Brachytherapy | Gynecological Applicator | Elekta. Accessed May 23, 2025. https://www.elekta.com/products/brachytherapy/geneva/

36. Jiang Y, Wang J, Jiang P, Wang X, Zhang L, Zhang Y. Clinical research of the value of high-risk CTV setting on intensity-modulated radiotherapy for stage IIB-IVA cervical cancer. *BMC Cancer*. 2023;23(1):481. doi:10.1186/s12885-023-10931-1

37. Use of image registration and fusion algorithms and techniques in radiotherapy: Report of the AAPM Radiation Therapy Committee Task Group No. 132 - Brock - 2017 - Medical Physics - Wiley Online Library. Accessed March 26, 2025. https://aapm.onlinelibrary.wiley.com/doi/10.1002/mp.12256

38. Rong Y, Rosu-Bubulac M, Benedict SH, et al. Rigid and Deformable Image Registration for Radiation Therapy: A Self-Study Evaluation Guide for NRG Oncology Clinical Trial Participation. *Pract Radiat Oncol*. 2021;11(4):282-298. doi:10.1016/j.prro.2021.02.007

39. Datteri RD, Dawant BM. Estimation and Reduction of Target Registration Error. *Med Image Comput Comput-Assist Interv MICCAI Int Conf Med Image Comput Comput-Assist Interv*. 2012;15(0 3):139-146.

40. Reinke A, Tizabi MD, Sudre CH, et al. Common Limitations of Image Processing Metrics: A Picture Story. Published online December 6, 2023. doi:10.48550/arXiv.2104.05642

41. Nenoff L, Amstutz F, Murr M, et al. Review and recommendations on deformable image registration uncertainties for radiotherapy applications. *Phys Med Biol*. 2023;68(24):24TR01. doi:10.1088/1361-6560/ad0d8a

42. Bender ET, Tomé WA. Utilization of consistency metrics for error analysis in deformable image registration. *Phys Med Biol*. 2009;54(18):5561-5577. doi:10.1088/0031-9155/54/18/014

43. Understanding Jacobian: Jacobian Matrix, Determinant and Examples. Testbook. Accessed May 21, 2025. https://testbook.com/maths/jacobian

44. Guo H, Wang J, Xia X, et al. The dosimetric impact of deep learning-based auto-segmentation of organs at risk on nasopharyngeal and rectal cancer. *Radiat Oncol*. 2021;16(1):113. doi:10.1186/s13014-021-01837-y

45. Brock KK, Mutic S, McNutt TR, Li H, Kessler ML. Use of image registration and fusion algorithms and techniques in radiotherapy: Report of the AAPM Radiation Therapy Committee Task Group No. 132. *Med Phys*. 2017;44(7):e43-e76. doi:10.1002/mp.12256

46. Euclidean Distance | Formula, Derivation & Solved Examples. GeeksforGeeks. 18:50:03+00:00. Accessed April 25, 2025. https://www.geeksforgeeks.org/euclidean-distance/

47. Zhong H, Kainz KK, Paulson ES. Evaluation and mitigation of deformable image registration uncertainties for MRI-guided adaptive radiotherapy. *J Appl Clin Med Phys*. 2024;25(6):e14358. doi:10.1002/acm2.14358

48. Abe T, Tamaki T, Makino S, et al. Assessing cumulative dose distributions in combined radiotherapy for cervical cancer using deformable image registration with pre-imaging preparations. *Radiat Oncol*. 2014;9(1):293. doi:10.1186/s13014-014-0293-4

49. Al-Rahamneh Z, Khtoom A, Ryalat M. Evaluation of Applying Surface Simplification Techniques in Medical Volume Data. *Int J Comput Appl*. 2021;183(9):7-11.